

1998

A kinetic study of the Ce(IV) oxidation of ethylene glycol

You-Peng Zhang
San Jose State University

Follow this and additional works at: https://scholarworks.sjsu.edu/etd_theses

Recommended Citation

Zhang, You-Peng, "A kinetic study of the Ce(IV) oxidation of ethylene glycol" (1998). *Master's Theses*. 1683.
DOI: <https://doi.org/10.31979/etd.p73d-phtt>
https://scholarworks.sjsu.edu/etd_theses/1683

This Thesis is brought to you for free and open access by the Master's Theses and Graduate Research at SJSU ScholarWorks. It has been accepted for inclusion in Master's Theses by an authorized administrator of SJSU ScholarWorks. For more information, please contact scholarworks@sjsu.edu.

INFORMATION TO USERS

This manuscript has been reproduced from the microfilm master. UMI films the text directly from the original or copy submitted. Thus, some thesis and dissertation copies are in typewriter face, while others may be from any type of computer printer.

The quality of this reproduction is dependent upon the quality of the copy submitted. Broken or indistinct print, colored or poor quality illustrations and photographs, print bleedthrough, substandard margins, and improper alignment can adversely affect reproduction.

In the unlikely event that the author did not send UMI a complete manuscript and there are missing pages, these will be noted. Also, if unauthorized copyright material had to be removed, a note will indicate the deletion.

Oversize materials (e.g., maps, drawings, charts) are reproduced by sectioning the original, beginning at the upper left-hand corner and continuing from left to right in equal sections with small overlaps. Each original is also photographed in one exposure and is included in reduced form at the back of the book.

Photographs included in the original manuscript have been reproduced xerographically in this copy. Higher quality 6" x 9" black and white photographic prints are available for any photographs or illustrations appearing in this copy for an additional charge. Contact UMI directly to order.

UMI

A Bell & Howell Information Company
300 North Zeeb Road, Ann Arbor MI 48106-1346 USA
313/761-4700 800/521-0600

**A KINETIC STUDY
OF THE Ce(IV) OXIDATION OF ETHYLENE GLYCOL**

A Thesis

Presented to

**The Faculty of the Department of Chemical and Materials Engineering
San Jose State University**

**In Partial Fulfillment
of the Requirements for the Degree
Master of Science**

by

You-Peng Zhang

May 1998

UMI Number: 1389694

UMI Microform 1389694
Copyright 1998, by UMI Company. All rights reserved.

**This microform edition is protected against unauthorized
copying under Title 17, United States Code.**

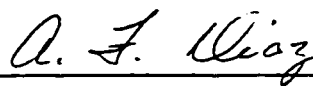
UMI
300 North Zeeb Road
Ann Arbor, MI 48103

© 1998

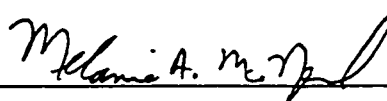
You-Peng Zhang

ALL RIGHTS RESERVED

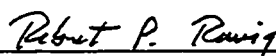
**APPROVED FOR THE DEPARTMENT OF
CHEMICAL AND MATERIALS ENGINEERING**

Handwritten signature of Dr. Arthur F. Diaz in cursive script.

Dr. Arthur F. Diaz

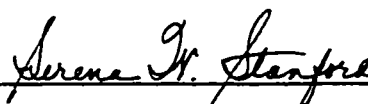
Handwritten signature of Dr. Melanie A. McNeil in cursive script.

Dr. Melanie A. McNeil

Handwritten signature of Dr. Robert P. Romig in cursive script.

Dr. Robert P. Romig

APPROVED FOR THE UNIVERSITY

Handwritten signature of Dr. Serena W. Stanford in cursive script.

Dr. Serena W. Stanford

ABSTRACT

A KINETIC STUDY OF THE Ce (IV) OXIDATION OF ETHYLENE GLYCOL

By You-Peng Zhang

The mediated electrochemical oxidation (MEO) technology is used for the removal of hazardous organic compounds in wastewater. In this process, a metal ion mediator generated by anodic oxidation serves as the oxidizing agent and oxidizes the organics to carbon dioxide and water. This study focused on the kinetics of the oxidation reaction of ethylene glycol (EG) in an aqueous Ce(IV) nitric acid solution. This reaction is a part of the overall MEO process and EG is selected as the prototype organic compound. This reaction was studied by measuring the change in the optical absorption at 350nm. The reaction was found to be first order with respect to $\text{Ce}(\text{NO}_3)_4$ and EG and apparent -1 order with respect to HNO_3 (for $[\text{HNO}_3] > 0.5\text{M}$). The second-order rate constant at 20°C was calculated equal to $0.228 [\text{HNO}_3] \text{ L}/(\text{mol}\cdot\text{s})$. The corresponding kinetic parameters E_a , ΔH^* , $\Delta G^*(20^\circ\text{C})$ and ΔS^* for the reaction were calculated equal to 10.0 Kcal/mol , 9.4 Kcal/mol , 22.2 Kcal/mol and $-43.7 \text{ Cal}/(\text{mol}\cdot^\circ\text{K})$, respectively.

Acknowledgement

I would like to thank all advisory committee members sincerely. I would like to give special thanks to my thesis advisor, Dr. Arthur F. Diaz, who guides and helps me through this research, provides the critical thinking and corrects the thesis writing. I would like to thank Dr. Melanie A. McNeil, who provided the instrument for my research. I would like to thank Dr. Robert P. Romig for his general support on this research.

As to my parents, I would like to show my deep appreciation for their financial support and concerns for all the previous years of my education.

TABLE OF CONTENTS

Chapter	Page
I. Introduction	1
1. Wastewater Treatment Process	1
2. Mediated electrochemical oxidation process	3
3. Motivation for study	6
II. Literature Review	7
III. Proposal	16
1. Hypothesis	16
2. Experimental Approach	16
3. UV-Visible Absorption Measurements	19
IV. Experimental Procedures	21
1. Chemicals	21
2. Calibration Curves	21
3. Room Temperature Kinetics	23
4. Kinetic Measurements at Elevated Temperatures	24

V. Results and Discussion	25
VI. Conclusions	49
VII. Suggestions for further study	50
References	51
Appendices	53

LIST OF TABLES

Table	Page
1. Thermodynamic parameters (Reference [5])	9
2. List of the stock solutions used in the kinetic measurements	22
3. Absorbance values at 350nm for several Ce (NO ₃) ₄ solutions	29
4. Absorbance values at 350nm for several Ce (NO ₃) ₃ solutions	29
5. Summary of reaction rate constants	32
6. Effect of [Ce(NO ₃) ₄] on the pseudo-first order rate constants	37
7. Effect of [EG] on the pseudo-first order rate constants	38
8. Effect of [HNO ₃] on the pseudo-first order rate constants	40
9. Comparison of thermodynamic parameters	46

LIST OF FIGURES

Figure	Page
1. Schematic of electrochemical cell	6
2. Plot of $\log k$ versus $\log [\text{PEG 400}]$ (Reference [5])	8
3. Verification of overall reaction order (Reference [5])	8
4. Absorption spectra of 0.2 mM $\text{Ce}(\text{NO}_3)_4$ /1.0M HNO_3	26
5. Absorption spectra of 0.8 mM $\text{Ce}(\text{NO}_3)_4$ /1.0M HNO_3	27
6. Absorption spectra of 0.2 mM $\text{Ce}(\text{NO}_3)_3$ /1.0M HNO_3	28
7. Absorbance of $\text{Ce}(\text{NO}_3)_4$ at 350nm with different $[\text{HNO}_3]$	30
8. Absorbance of $\text{Ce}(\text{NO}_3)_3$ at 350nm with different $[\text{HNO}_3]$	31
9. Plot of $\ln(1/(1-X))$ versus time (Aliquot method)	35
10. Plot of $\ln(1/(1-X))$ versus time (Single Sample method)	36
11. Plot of $\log k'$ against $\log [\text{EG}]$	39
12. Plot of $\log k'$ against $\log [\text{HNO}_3]$	41
13. Plot of $\ln(a(b-x)/b(a-x))$ against time	42
14. Plot of $\ln(a(b-x)/b(a-0.1x))$ against time	44
15. Plot of $\ln k_2$ versus $1/T$	46
16. Plot of $\ln(a(b-x)/b(a-0.5x))$ against time	57

Chapter I

Introduction

1. Wastewater Treatment Processes

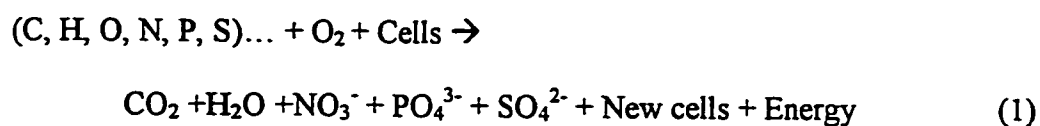
Wastewater, the water discarded after it has been used for domestic, commercial, agricultural or industrial purposes, usually requires some treatment before discharge, to protect the receiving environment. The main objective of wastewater treatments is to remove undesirable impurities from the finished water. The choice of treatment for a particular wastewater depends on the physical, chemical and biological characteristics of the impurities to be removed [1]. Wastewater treatment technology has accelerated in recent decades. In particular, the treatment of solid and liquid hazardous organic compounds in wastewater is under increased observation.

Wastewaters from different industrial processes differ widely in their composition and contaminant concentration levels depending on the industry. For example, in the production of raw materials for the dye industry, aniline and nitrobenzene are produced and discharged to wastewater. In the production of organic solvents, propyl acetates and chlorinated compounds are presented in the wastewater. Hence, different treatment methods are required to treat different contaminants [2]. Some examples of treatment processes are as follows:

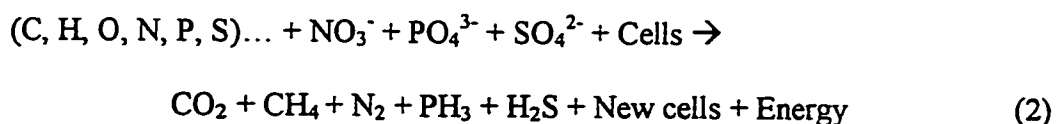
Physical treatment processes are generally the simplest form of treatment and consist of processes such as screening, sedimentation, filtration and flotation. Suspended and

floating organic solids can be separated through these mechanical operations, but dissolved organics still remain in the treated wastewater.

Biological treatment processes can be effective for removing organic contaminants since they can often be degraded. This treatment includes aerobic biological processes and anaerobic biological processes, depending on the presence or absence of oxygen in wastewater. If free dissolved oxygen is present in the water phase and is utilized by the microorganisms to degrade the organic compounds, the processes are termed aerobic. The general expression is shown in Equation 1. The products of the aerobic processes are not usually objectionable.



If the microorganisms utilize bound oxygen from inorganic salts to degrade the organic compounds, the processes are termed anaerobic. The general expression is shown in Equation 2.



In addition, the biodegradation of organic contaminants may be carried out by the heterotrophic organisms, which utilize organic carbon as their energy source to break down organic contaminants. A biological treatment is only used with wastewater which does not contain organic refractory compounds (refractory compounds refer to those compounds with high melting points) and where sufficient reaction time can be allowed to complete reaction [2].

Chemical treatment processes can successfully alter the nature of a substance so that the products formed in the processes are no longer objectionable in the finished water. The processes mainly include coagulation, flocculation and oxidation processes to treat organic contaminants. Among these processes, the chemical oxidation processes are the most important. Oxidants, such as chlorine, chlorine dioxide, ozone and potassium permanganate, are used to oxidize the organic compounds in wastewater. This treatment can be used to disinfect water, control taste and odor, remove color and algae, and reduce iron and manganate contents. It is especially effective in the removal of the refractory organic compounds. However, ozone is expensive, and chlorine can react with organic materials in wastewater and produce trihalo-methanes (THMs). These products are undesirable and difficult to remove from the finished water [2].

Adsorption treatment process uses activated carbon to remove the organic contaminants from wastewater. In general, pore structure and the high surface area of carbon are the most important considerations for evaluating the efficiency of this treatment process. It can also remove refractory organic compounds from wastewater. However, the costs of manufacture and regeneration of the activated carbon are very high [3].

2. Mediated electrochemical oxidation (MEO) process

The mediated electrochemical oxidation (MEO) process is a newer developing technology. It is an electrochemical oxidation process, which uses the oxidizing power of a metal ion mediator to oxidize organic compounds in wastewater. This process can be

used to treat wastewater containing refractory organic compounds. The primary advantages of this technology are:

- (i) The process operates in an electrochemical cell, which can completely converted the organic contaminants to carbon dioxide and water.
- (ii) Wastewater streams containing low amounts of organic contaminants can be treated.

However, this new process still needs advanced studies [4].

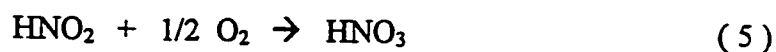
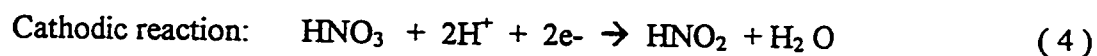
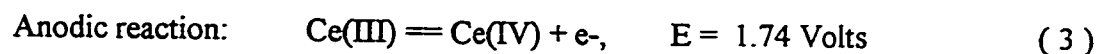
The mediated electrochemical oxidation (MEO) process involves the anodic activation of a metal ion mediator in an aqueous electrolyte, which then oxidizes the organic contaminates to CO_2 and H_2O . The metal ion mediator is then recycled at the anode surface.

The mediator plays an important role in the electrochemical reaction process. Silver [Ag(II)], cobalt [Co(III)] and cerium [Ce(IV)] have been selected for use as mediators because these redox pairs have high oxidation potentials. Ag(II)/Ag(I) has $E = 1.98\text{V}$, Co(III)/Co(II) has $E = 1.83\text{-}1.92\text{V}$, and Ce(IV)/Ce(III) has $E = 1.74\text{V}$. These values are suitable for the oxidation of organic contaminates.

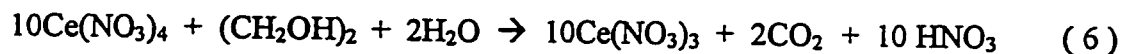
There are serious disadvantages in the Ag(II)-based process. These include the precipitation of Ag as a halide salt by anions liberated during the destruction of halogenated organics, leakage of large quantities of Ag through the electrode separator, excessive corrosion of the anode in the presence of HNO_3 and HCl , and generation of HNO_2 and NO_x at the cathode.

In the Co(III)-based and Ce(IV)-based processes, the above problems are not present, but since cobalt and cerium have relatively lower oxidation potentials, they are not suited for the total oxidation of some organic substances, such as superchlorinated organics [4].

The mediated electrochemical oxidation process uses the regenerative oxidant / mediator, Ce(III)/ Ce(IV) couple in an electrochemical cell to oxidize ethylene glycol (EG) completely to carbon dioxide and water. The soluble cerium mediator, Ce(IV), is generated from Ce(III) at the anode, Equation 3. This anodic reaction is balanced by the cathodic reduction of nitric acid to nitrous acid, Equation 4. But HNO₃ can be regenerated by the chemical reaction of HNO₂ with oxygen, Equation 5. In the bulk anolyte solution, Ce(IV) reacts with EG, Equation 6. This reaction has a stoichiometry of 10 moles Ce(IV) to 1 mole EG. The generated Ce(III) is recycled to Ce(IV) to repeat the oxidation / reduction cycle. A schematic for this process is shown in Figure 1.



Solution reaction:



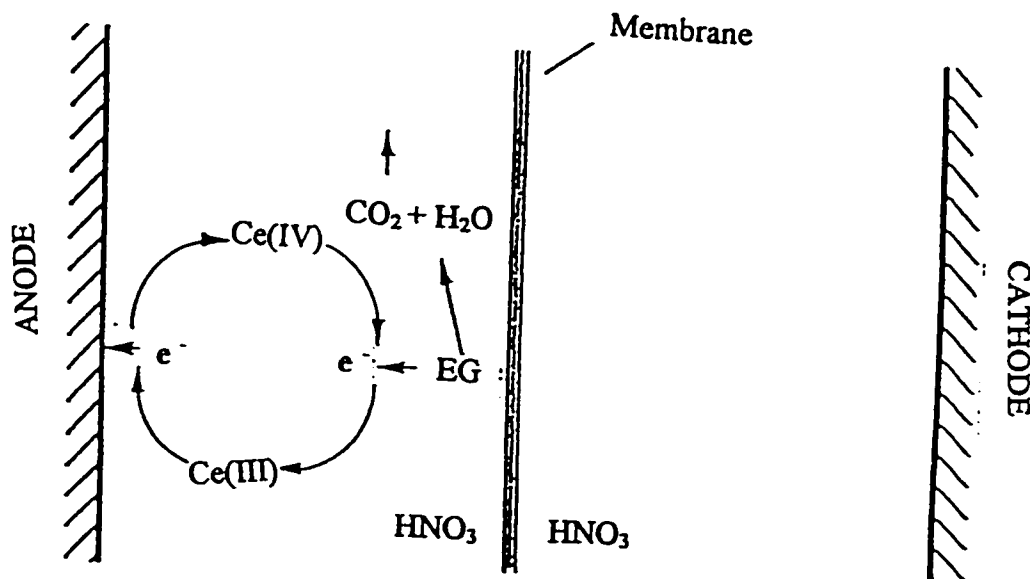


Figure 1. Schematic of the Electrochemical Cell.

3. Motivation for Study

Temperature is an important operating parameter in any practical wastewater clean-up processes, because it can be used to control the time for a complete reaction. This study focused on determining the effect of temperature on the oxidation reaction of EG by $\text{Ce}(\text{NO}_3)_4$ in aqueous nitric acid. The reaction order and the reaction constant will be determined first at room temperature, and then the rate constants will be determined at higher temperatures. These rate constants can be used to calculate the kinetic parameters: E_a , ΔH^* , ΔS^* and ΔG^* . All of these data are useful for calculating the reaction time for the completion of the reaction, and helpful in designing the wastewater clean-up processes.

Chapter II

Literature Review

Nagarajan et al. [5] studied the kinetics of oxidation reaction of poly(ethylene glycol) (PEG) by ceric sulphate in aqueous sulphuric acid. This reaction was studied at 26°C only. The rate of the reaction was determined by following the disappearance of Ce(IV) with time by measuring optical density change at 304nm using an UV-visible spectrophotometer. At this wavelength, all other reactants and products had negligible absorption. The kinetic experiments were made with excess PEG so that the reactions would be pseudo- first-order with respect to Ce(IV). The pseudo- first-order kinetic plots showed excellent linearity. Therefore, the rate of oxidation depended directly on [Ce(IV)] and [PEG]. At constant pH and in the presence of excess PEG, the reaction was shown to be first-order with respect to [Ce(IV)]. Pseudo- first-order rate constants were calculated from $t_{1/2}$ values obtained from plots of the log (optical density) versus time using the relationship:

$$k = 0.693 / t_{1/2} \quad [\text{time}]^{-1} \quad (7)$$

The plot of log k against log [PEG] gave a straight line with a slope of unity. This is shown in Figure 2 for a solution containing 0.15mM Ce(IV), 0.05M H₂SO₄. Hence the linear fit demonstrated that the reaction was first order with respect to [PEG] and the overall order of this reaction was two at constant pH. This was verified further by plotting $\log\{(b-x)/(a-x)\}$ against time. This is shown in Figure 3 for a solution containing 0.0774mM Ce(IV), 1.5 mM PEG, 0.05M H₂SO₄ and $\mu=1.05M$ at 26°C. At constant pH,

the plot had a good linear fit in 60 minutes. Even though the plot deviated from linearity after 60 minutes, it still demonstrated that the overall reaction was a second order since the reaction had completed 99.9% in 60 minutes.

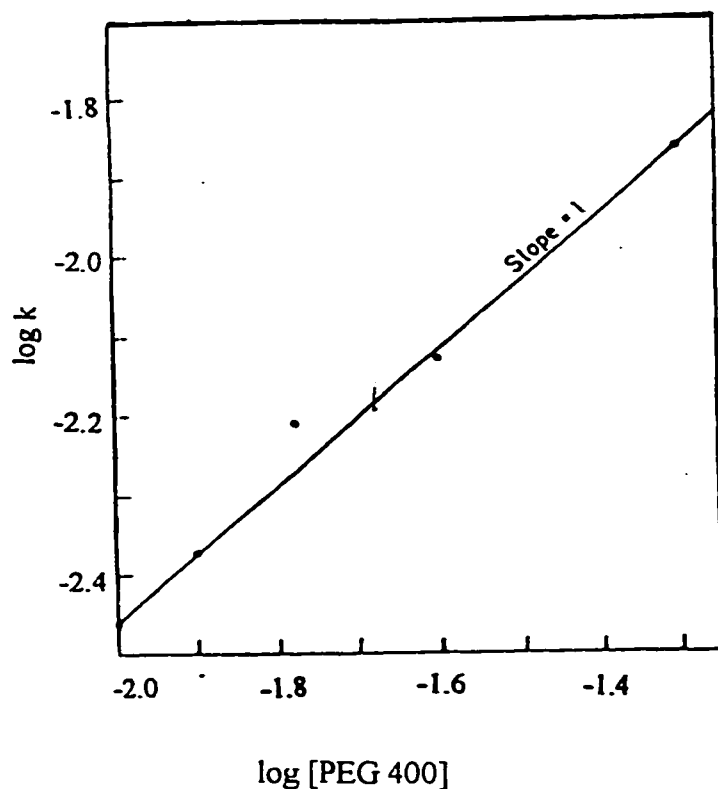


Figure 2. Plot of $\log k$ against $\log [\text{PEG 400}]$ for a solution containing 0.15mM Ce(IV), 0.1M H^+ and $\mu=1.05\text{M}$ at 26°C. (Recreated from Reference [5])

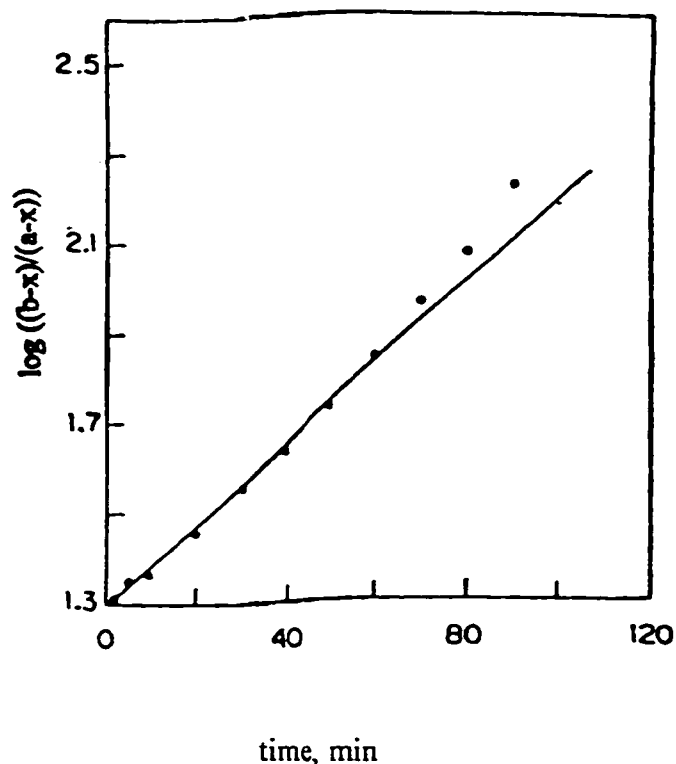


Figure 3. Plot of $\log \{(b-x)/(a-x)\}$ against time for a solution containing 0.0774mM Ce(IV), 1.5mM PEG 400, 0.1 M H^+ and $\mu=1.05\text{M}$ at 26°C. (Recreated from Reference [5])

Although the temperature effect on the oxidation reaction rate was not discussed, the thermodynamic parameters were provided for a solution containing 2mM PEG, 0.15mM Ce(IV) and 0.1M H₂SO₄. These data provided by the authors are summarized in Table 1.

Table 1. Thermodynamic parameters measurements using solutions containing 2mM PEG, 0.15mM Ce(IV) in 0.05M H₂SO₄ ($\mu=1.05\text{M}$).

Substrate	E _a , Kcal/mol	ΔG° , Kcal/mol	ΔH° , Kcal/mol	ΔS° , Cal/(mol.K)
PEG400	10.49	24.07	9.86	-47.22
PEG4000	9.81	21.84	9.22	-43.04
PEG6000	8.58	20.45	8.00	-42.50

Regarding the mechanism of the oxidation reaction, the authors assumed that Ce(IV) and PEG reacted to form a transition state which then quickly decomposed to produce an organic radical intermediate, Ce(III) and a proton. These two steps together were the rate-determining step. The radical intermediate then reacted with one more Ce(IV) and quickly produced the products of the reaction without the formation of any stable intermediate complexes.



The kinetic expression given for this reaction is shown in Equation 8. The acid concentration appeared in this expression, and the reaction rate decreased directly with an

increase in $[\text{H}_2\text{SO}_4]$. However, an increase of $[\text{H}_2\text{SO}_4]$ accelerated the reaction rate when the ionic strength of the solution was kept constant.

$$\text{Rate} = K'[\text{PEG}][\text{Ce(IV)}]/[\text{H}_2\text{SO}_4] \quad (8)$$

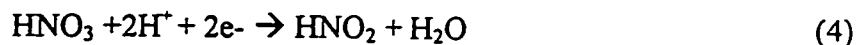
Nagarajan et al. [5] successfully studied the kinetic and mechanistic aspects of the oxidation of PEG by Ce(IV) in aqueous sulphuric acid. The reaction orders and the kinetic expression were obtained. Their work mainly focused on a qualitative investigation and neglected the detailed calculations. Data on the temperature effect and the rate constants at other temperatures were not reported.

Farmer et al. [7] studied the Ag(II) mediator electrochemical oxidation of ethylene glycol (EG) in a nitric acid solution. They demonstrated the complete conversion of EG to CO_2 and developed an understanding of the reaction intermediates and mechanism.

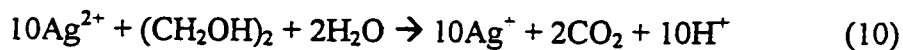
Ag(II) was generated by the anodic oxidation of Ag(I)



In the absence of organics in solution, most of the Ag(II) was present as a dark brown nitrate complex, AgNO_3^+ . This reaction was accompanied by the cathodic reduction of nitric acid

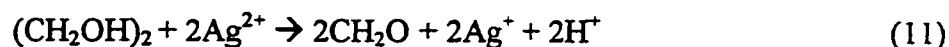


The complete oxidation of EG by Ag(II) was represented by

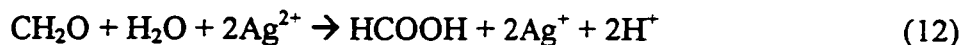


They found that formaldehyde and formic acid were the two primary intermediates formed during the conversion of EG to CO₂. The total ion chromatogram (TIC) of an unextracted anolyte sample taken during the partial oxidation of EG showed the presence of CO₂, N₂O and formaldehyde which eluted together during 1.8-3.8 minutes and formic acid at 43.52 minutes.

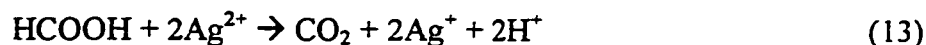
They postulated that the complete oxidation of EG occurred in three steps. They called this “mechanism” of the reaction. First, the oxidation of EG by Ag (II) generated two molecules of formaldehyde or an aldehyde-like intermediate.



Second, this intermediate was oxidized by Ag(II) to produce formic acid.



Third, the formic acid was oxidized to CO₂.



Ten Ag(II) ions (10 electrons) were required to completely oxidize one EG molecule to CO₂.

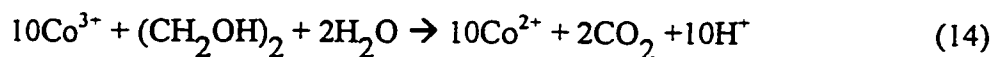
EG and its intermediates were oxidized by Ag(II) near the surface of the rotating cylinder anode. As a result, the anolyte remained clear during the oxidation of EG, indicating that the bulk Ag(II) concentration was essentially zero. The anolyte turned dark brown after complete conversion of EG to CO₂, which indicated that a significant concentration of Ag(II) had developed in the bulk anolyte.

These experiments were performed at three temperatures: 27°C, 33°C and approximate 46°C. The elevations of the anolyte temperature above ambient were due to

ohmic heating in the cell and not due to a deliberate temperature control. The reaction orders of each reactant and the overall reaction order were not discussed and the kinetic expression of the reaction could not be obtained.

Farmer et al.[8] studied the Co(III) mediated electrochemical oxidation of EG in aqueous sulphuric acid. By using a rotating cylinder anode in the electrochemical reactor and measuring the rate of CO₂ generation, they demonstrated the complete conversion of EG to CO₂.

Co(III) was generated by the anodic oxidation of Co(II) and was reduced by reactions with EG. The complete reaction of Co(III) with EG was represented by Equation 14,



The authors described the following steps in the complete reaction of EG by Co(III). The Co(III) oxidation of EG generated two molecules of formaldehyde or an aldehyde-like intermediate. These intermediates were then oxidized to formic acid. The last step was the oxidation of formic acid to CO₂. Ten Co(III) ions (10 electrons) were required for complete oxidation of one EG molecule. This sequence of steps was described as the “mechanism” of the reaction.

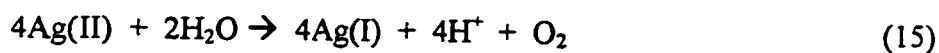
EG and its intermediate were oxidized by Co(III) near the surface of the anode. During the oxidation reaction, the color of the bulk anolyte was light pink, characteristic of Co(II) solutions (peak absorbance at 513 nm), indicating that the concentration of

Co(III) in the bulk anolyte was essentially zero. After complete conversion of EG to CO₂, the solution turned dark purple, characteristic of Co(III) solutions (peak absorbance at 342 nm).

These experiments were also performed at three temperatures: 27°C, 33°C and approximate 46°C. The report had very little kinetic data and no information on the temperature effect on the reaction rate.

Bringmann et al.[4] studied the mediated electrochemical oxidation of chlorinated hydrocarbons with Ag(II), Co(III) and Ce(IV) as mediators and compared their oxidizing capabilities. From the total oxidation experiments at room temperature, they showed that the Ag(II) mediator destroyed even superchlorinated organic substances such as pentachlorophenol (PCP), Lindane and polychlorinated biphenyls (PCBs). High degradation rates could be obtained. Co(III) was a suitable mediator for the total oxidation of compounds with a certain chlorination grade, such as tetrachloro-benzene. However, PCP, PCBs and Lindane could not be oxidized completely. Ce(IV) was not suitable for the total oxidation of superchlorinated organics because the low oxidation potential of Ce(III) / Ce(IV), (E=1.74V). But it could be used for the partial oxidation of organic substances.

The authors also studied the oxidation of water by Ag(II) ions and Co(III) ions in aqueous media using the rotating disc electrode at various temperatures. The overall reaction of Ag(II) with water was shown in Equation 15,



The second-order expression for this reaction was as shown in Equation 16,

$$\text{Rate} = k_{II}[\text{Ag(II)}]^2 \quad (16)$$

Three reports [9 -11] described the kinetics / electrochemical investigations related to the development of a wet scrubbing process for SO₂/ NO_x abatement from industrial waste gases and using Ce(IV) as an oxidizing agent. For the oxidation of SO₂ by Ce(IV) in a aqueous sulfuric acid solution, Nzikou et al. [9] showed that the charge transfer coefficients were weakly affected by the [H₂SO₄] up to 5M, however the diffusion coefficients and the rate constants decreased as [H₂SO₄] increased. Auroussean et al. [10] found that this reaction was first-order with respect to each of the reactants, and the global rate constant for SO₂ consumption decreased with increasing [H₂SO₄]. Auroussean et al. [11] also studied the oxidation of nitrogen oxides in ceric solution accomplished by the liquid-phase oxidation of nitrous acid. They also found that this oxidation was first-order with respect to Ce(IV) and to nitrous acid. The wet air oxidation process was reported in paper [12]. This process operates at high temperature (125-320°C) and pressure (0.5 -20 MPa) conditions and is useful for the treatment of hazardous, toxic and non-biodegradable wastewater. Many industrial applications were presented using this technology [12].

A survey of the literature contained many studies with different mediators for the electrochemical oxidation reactions. These studies mainly focused on analyzing the formation of the intermediates in the reactions and describing the corresponding

mechanisms [4, 5-8]. These “mechanisms” are basically a description of the reaction steps in the overall reaction and are not reaction mechanisms. The quantitative effect of the temperature was briefly mentioned in one paper [5]. Temperature is an important operating parameter in the practical wastewater clean-up processes, and its effect must be quantified to determine the reaction time required for the complete conversion of contaminants.

Chapter III

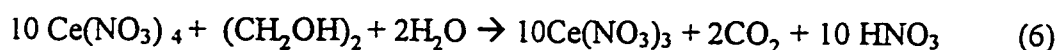
Proposal

1. Hypothesis

This research is to verify the hypothesis that the oxidation reaction of ethylene glycol (EG) by ceric nitrate ($\text{Ce}(\text{NO}_3)_4$) in aqueous nitric acid is first order with respect to each reactant, and to verify that the reaction is an activated process in which reaction rate increases with temperature. The reaction rate obeys the Arrhenius Equation and can be parameterized to provide the information needed to determine the reaction times in the wastewater treatment processes.

2. Experimental Approach

The complete oxidation reaction of EG by $\text{Ce}(\text{NO}_3)_4$ in aqueous nitric acid shown in Equation 6 has a stoichiometry of 10 moles $\text{Ce}(\text{NO}_3)_4$ to 1 mole $(\text{CH}_2\text{OH})_2$.



However, the kinetic reaction order can differ from this stoichiometry and must be verified.

The oxidation reaction of poly (ethylene glycol) (PEG) by ceric sulphate in aqueous sulphuric acid was studied by Nagarajan et al. [5]. The data from their study were used to design experiments to study the oxidation reaction of EG by $\text{Ce}(\text{NO}_3)_4$ in nitric acid solution. The PEG reaction was reported to be second order overall, i.e., first order with

respect to each reactant at constant $[H_2SO_4]$. The kinetic expression is shown in Equation 17 where $m=1$ and $n=1$,

$$-d [Ce(NO_3)_4] / dt = k_2 [Ce(NO_3)_4]^m [EG]^n \quad (17)$$

and the corresponding integrated form is,

$$k_2 t = \{1/([Ce(NO_3)_4]_0 - [EG]_0)\} \ln\{[EG]_0[Ce(NO_3)_4]_t / [Ce(NO_3)_4]_0[EG]_t\}$$

or the general kinetic expression,

$$k_2 t = \{1/(a-b)\} \ln \{b(a-x) / a(b-x)\} \quad (18)$$

where a is $[Ce(NO_3)_4]_0$, b is $[EG]_0$ and x is the quantity of $Ce(NO_3)_4$ reacted at time t .

The reaction order for each reactant can be determined using the first-order approximation method. This method provides the pseudo-first-order rate constants and can be applicable when the concentration of one of the reactants greatly exceeds the other and does not vary significantly during the reaction. Under conditions where the reaction solution contains excess EG, the rate expression in Equation 17 becomes

$$-d [Ce(NO_3)_4] / dt = k' [Ce(NO_3)_4]^m \quad \text{where } k' = k_2 [EG]_0^n \quad (19)$$

When $m = 1$, the integrated form of Equation 19 is,

$$\ln \{[Ce(NO_3)_4]_0 / [Ce(NO_3)_4]_t\} = k't \quad (20)$$

This expression can be written in terms of X , the extent of reaction, where,

$$X = \{[Ce(NO_3)_4]_0 - [Ce(NO_3)_4]_t\} / [Ce(NO_3)_4]_0$$

and $[Ce(NO_3)_4]_t$ is given by,

$$[Ce(NO_3)_4]_t = [Ce(NO_3)_4]_0 (1 - X) \quad (21)$$

Equation 20 becomes,

$$\ln [1 / (1-X)] = k't \quad (22)$$

This first order rate expression can be used to determine k' , and the order (n) with respect to EG is determined by the slope of a plot of $\log k'$ versus $\log [EG]$.

Alternatively, the reaction rate can be measured in a solution containing excess $Ce(NO_3)_4$. In this case, the rate expression is approximated by

$$-d[Ce(NO_3)_4]/dt = k'' [EG]^n \quad \text{where } k'' = k_2 [Ce(NO_3)_4]^m \quad (23)$$

Similarly, this expression can be used to determine k'' , and the order (m) can be determined from the slope of a plot of $\log k''$ versus $\log [Ce(NO_3)_4]$.

The relationship between k' and temperature is given by the Arrhenius Equation,

$$\ln k' = \ln A - E_a / RT \quad (24)$$

and the activation energy (E_a) can be obtained from the slope of a plot of $\ln k'$ versus $1/T$. The transition state kinetic parameters can then be calculated using the following equations [13].

$$\Delta H^* = E_a - RT \quad (25)$$

$$k = (kT/h) \exp(-\Delta G^*/RT) \quad (26)$$

$$k = (kT/h) \exp(\Delta S^*/R) \exp(-\Delta H^*/RT) \quad (27)$$

where k = the reaction rate constant at room temperature, $T(^{\circ}K)$,

k = Boltzmann constant = $1.381 \times 10^{-23} \text{ J/^{\circ}K}$,

h = Planck constant = $6.626 \times 10^{-34} \text{ J}\cdot\text{s}$.

3. UV-Visible Absorption Measurements

In these kinetic experiments, the reaction rate was followed by the change in the $\text{Ce}(\text{NO}_3)_4$ absorbance at 350nm with time using an UV-Visible absorbance spectrophotometer. A HP 8452A diode array spectrophotometer was used. A HP 89530A Ms-Dos UV/Vis software system was set up to provide qualitative analysis of spectra and quantitative values of absorbance at 350nm.

The absorption is related to the concentration by the Lambert - Beer's Law [15],

$$\text{Abs} = \log (I_0 / I) = \epsilon l c \quad (28)$$

where Abs = absorbance,

$I_0 (I)$ = the intensity of the light entering (emerging from) the sample,

ϵ = the molar extinction coefficient, cm^2/mol

l = the sample thickness, l cm

c = the concentration of the light - absorbing substance, moles/ cm^3

The absorbance of solutions with different $[\text{Ce}(\text{NO}_3)_4]$ and $[\text{Ce}(\text{NO}_3)_3]$ were measured individually to establish the calibration curves of absorbance versus concentration. With these calibration curves, the absorbance values could be used directly in the kinetic calculations in place of concentrations. Hence, the rate expressions are written in terms of the absorbance (Abs) using the definitions tabulated below, considering $C_0 = C_f$ and X is the extent of the reaction.

Time (t)	[Ce(NO ₃) ₄]	[Ce(NO ₃) ₃]	Solution Absorbance(Abs)
0	C _o	0	(Abs) _o = e ₁ lC _o
t	C _o (1-X)	C _f X	(Abs) _t = e ₁ lC _o (1-X) + e ₂ lC _f X
∞	0	C _f	(Abs) _f = e ₂ lC _f

Therefore, X is given by,

$$X = [(Abs)_o - (Abs)_t] / [(Abs)_o - (Abs)_f] \quad (29)$$

and Equation 22 can be written in terms of the absorbance as follows,

$$\ln[(Abs)_o - (Abs)_f] / [(Abs)_t - (Abs)_f] = k' * t \quad (30)$$

In this study, X was calculated according to Equation 29, then the $\ln (1/(1-X))$ values were obtained. The pseudo-first-order rate constants (k's) were obtained from the slopes in the plots of $\ln (1/(1-X))$ versus time using the relationship indicated by Equation 22. Standard linear and second-order least squares fits were used to determine the average value and the deviation. The second-order rate constant (k₂) was given by k'/[EG]_o.

Chapter IV

Experimental Procedures

1. Chemicals

Stock solutions of 1.5M ceric nitrate ($\text{Ce}(\text{NO}_3)_4$) and 2.6M cerous nitrate ($\text{Ce}(\text{NO}_3)_3$) were used as received. These were individually diluted with 0.2M, 0.5M, 1.0M and 2.0M HNO_3 to the desired concentrations for the second set of stock solutions. Concentrated HNO_3 (15.8M) from Fisher Scientific Co. was diluted with distilled water to prepare the 0.2M, 0.5M, 1.0M and 2.0M standard solutions. The concentrations of these solutions were determined by titration with 1.0M NaOH. Ethylene glycol (EG, 99.9 wt.%) was used as received. Triple distilled water was used for the preparation of all the solutions. Table 2 lists the second set of stock solutions prepared for the kinetic measurements.

2. Calibration Curves

The absorption spectra in the region from 300nm to 450nm were recorded for the second set solutions of $\text{Ce}(\text{NO}_3)_4$, $\text{Ce}(\text{NO}_3)_3$, EG in HNO_3 solutions. The absorbance at 350nm was selected for the analytical measurements and was recorded for five solutions containing 0.1mM, 0.2mM, 0.4mM, 0.6mM and 0.8mM $\text{Ce}(\text{NO}_3)_4$ each. These values were used to establish the absorbance-concentration calibration curve of $\text{Ce}(\text{NO}_3)_4$. The linearity of the relationship was determined using standard linear and second-order least squares fits. The same procedure was used to obtain the calibration curve for $\text{Ce}(\text{NO}_3)_3$.

Table 2. List of the stock solutions* used in the kinetic measurements

Run	[Ce(NO ₃) ₄], mM	[EG], mM	[HNO ₃], M	Ratio**
1, 2, 3	0.20	3.0	4.0	15.0
4, 5	0.40	3.0	4.0	7.5
6, 7	0.20	6.0	4.0	30.0
8, 9	0.20	3.0	2.0	15.0
10,11	0.40	3.0	2.0	7.5
12,13	0.80	3.0	2.0	3.8
14,15	1.00	3.0	2.0	3.0
16,17	0.20	6.0	2.0	30.0
18,19	0.20	9.0	2.0	45.0
20,21	0.20	12.0	2.0	60.0
22,23	0.20	3.0	1.0	15.0
24,25	0.20	3.0	0.4	15.0
26	0.80	1.5	2.0	1.9
27,28	0.20	3.0	4.0	15.0
29,30	0.20	3.0	4.0	15.0

Note: * The concentration values indicate the second set of stock solutions.

** The ratio refers to [EG]:[Ce(NO₃)₄].

The reaction rate was followed measuring the change in the absorbance at 350nm with time and the calibration curves were used to calculate the rate constants.

3. Room Temperature Kinetics

The oxidation reaction rates were studied at room temperature (20 ± 2 °C). The kinetic experiments were carried out using excess EG to apply the pseudo-first-order kinetic treatment with respect to $\text{Ce}(\text{NO}_3)_4$. The reaction was initiated when 50ml of 0.2mM $\text{Ce}(\text{NO}_3)_4$ / 4.0M HNO_3 was added to 50ml of 3.0mM EG in a 250ml reaction flask.

3.1 Aliquot method: At each suitable time interval, a portion of the reaction mixture was transferred to a 1cm UV quartz cell and the absorbance at 350nm was recorded. After each measurement, the solution in the cell was discarded. The time of the first measurement was taken as the initial time ($t = 0$). This procedure was repeated at designated times and the absorbance at each time interval was recorded. The end of the reaction was determined when the absorbance value was nearly equal to the absorbance of 0.1mM $\text{Ce}(\text{NO}_3)_3$ / 2.0M HNO_3 medium. This time interval was confirmed by the number of the reaction half-life.

3.2 Single sample method: A portion of the reaction mixture was transferred to a 1cm UV quartz cell and left there for the duration of the run. In this case the 1cm UV quartz cell

was the reactor. At each suitable time interval, the absorbance of the solution at 350nm was recorded. The end of the reaction was determined as above.

4. Kinetic Measurements at Elevated Temperatures

The kinetic measurements at 40°C and 60°C were performed using the aliquot method. The reaction solutions containing 0.2mM $\text{Ce}(\text{NO}_3)_4$ / 4.0M HNO_3 and 3.0mM EG were used. The reactor for the temperature studies was a 250ml three-necked flask. This flask was heated with a heating mantle and the temperature was pre-set with a transformer. One of the two side necks was equipped with a thermometer and the other was plugged with a glass stopper. The central neck was used to take the samples. Water was first heated in the flask to set the desired temperature, and the transformer indicator was fixed. The water was then discarded and 50ml of 0.2mM $\text{Ce}(\text{NO}_3)_4$ / 4.0M HNO_3 and 50 ml of 3.0mM EG were added into the flask. After 2 minutes, an aliquot was transferred to the 1cm UV quartz cell and the cell was immersed in icewater for one minute. The cell was then allowed to warm towards room temperature while being held in hand for one minute before recording the absorbance values. The time of the first measurement was taken as the initial time ($t = 0$) and the corresponding absorbance was recorded. This procedure was repeated with each subsequent aliquot. This procedure was used consistently to minimize errors due to the reaction progress, which may have occurred during the sample handling and analysis.

Chapter V

Results and Discussion

The absorption maxima of $\text{Ce}(\text{NO}_3)_4$ varied slightly with the solution concentrations. For example, the absorption maximum appeared at $(331 \pm 1 \text{ nm})$ for the 0.8 mM $\text{Ce}(\text{NO}_3)_4$ /1.0M HNO_3 solution and at $(327 \pm 1 \text{ nm})$ for the 0.2 mM $\text{Ce}(\text{NO}_3)_4$ /1.0M HNO_3 . The absorption maxima of $\text{Ce}(\text{NO}_3)_3$ appeared at 324nm independent of the concentration. These spectra are shown in Figures 4, 5, and 6. 350nm was selected as the analytical wavelength for the measurements because it provided the maximum difference of the $\text{Ce}(\text{NO}_3)_4$ - $\text{Ce}(\text{NO}_3)_3$ absorbances, whereas all the other reactants and products had negligible absorption.

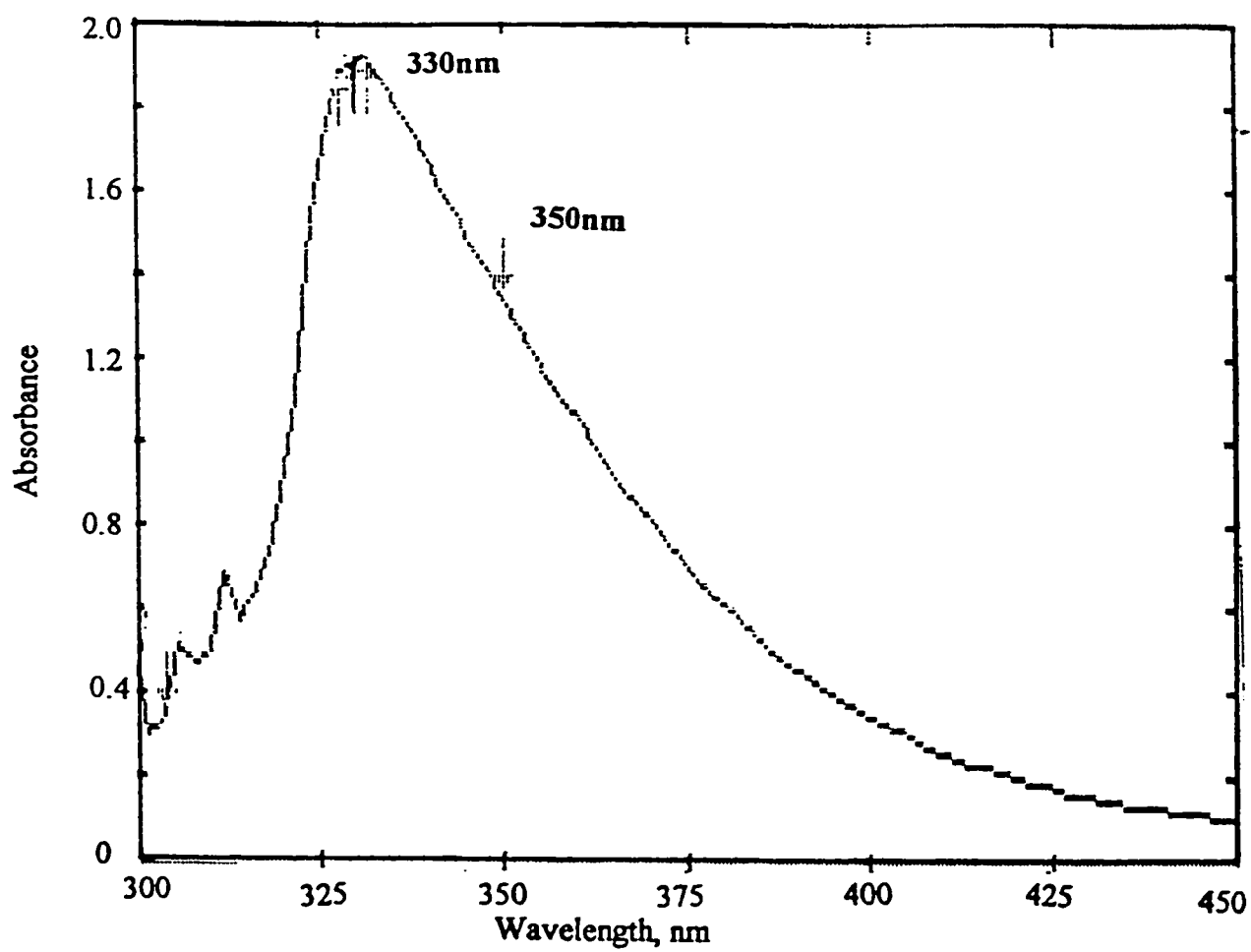


Figure 4. Absorbance spectra of 0.8 mM $\text{Ce}(\text{NO}_3)_4$ / 1.0 M HNO_3 solution.

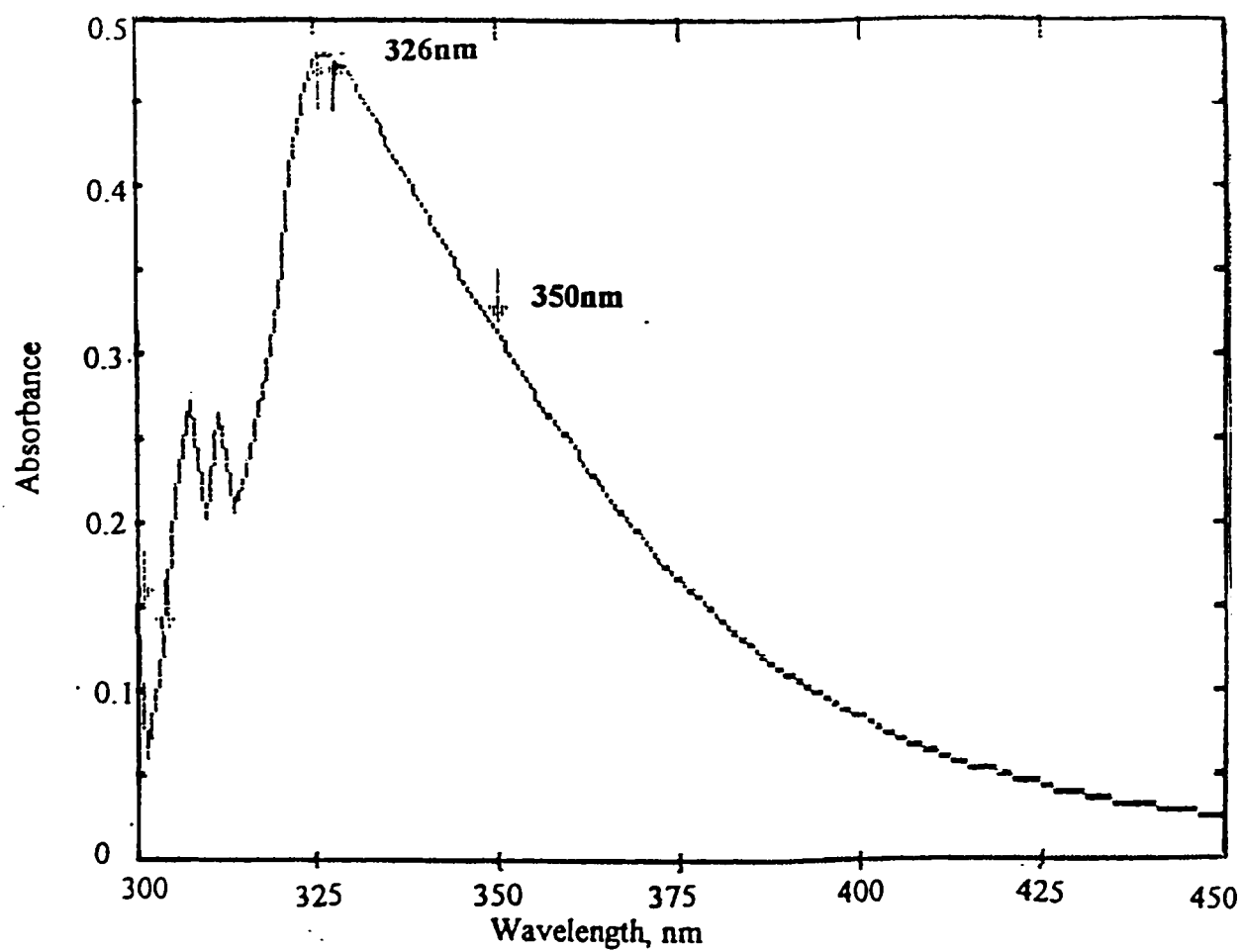


Figure 5. Absorbance spectra of 0.2 mM $\text{Ce}(\text{NO}_3)_4$ / 1.0 M HNO_3 solution.

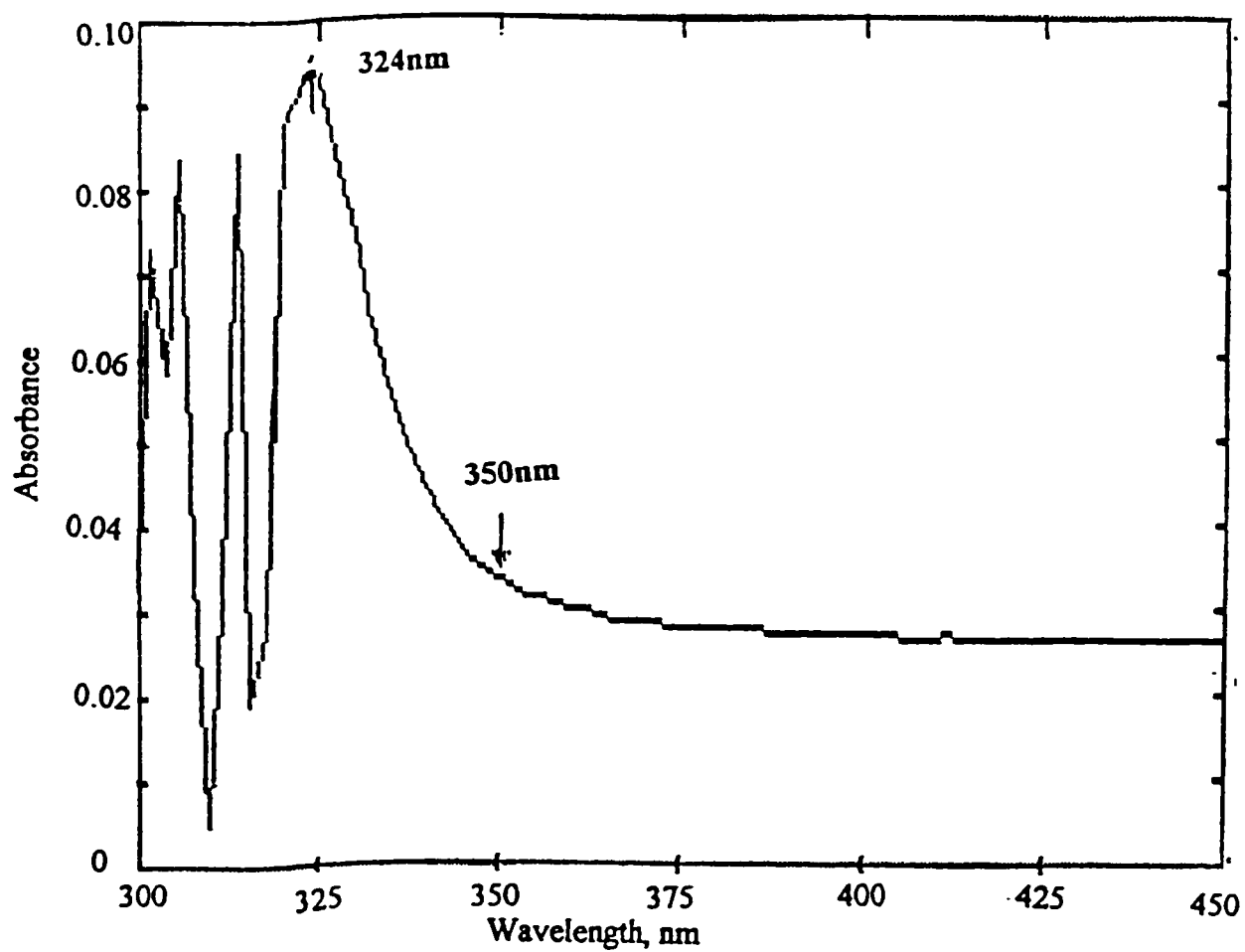


Figure 6. Absorbance spectra of 0.2 mM $\text{Ce}(\text{NO}_3)_3$ / 1.0 M HNO_3 solution.

The plots in Figures 7 and 8 show that the calibration curves have good linearity extrapolate to zero and depend on $[\text{HNO}_3]$. The absorbance values and the slopes of the plots are summarized in Tables 3 and 4. The linear relationship for $\text{Ce}(\text{NO}_3)_4$ is: $\text{Abs(IV)} = \text{slope} [\text{Ce}(\text{NO}_3)_4]$ and for $\text{Ce}(\text{NO}_3)_3$ is: $\text{Abs(III)} = \text{slope} [\text{Ce}(\text{NO}_3)_3]$. It can be seen in Tables 3 and 4 that at constant $[\text{Ce}(\text{NO}_3)_4]$ and $[\text{Ce}(\text{NO}_3)_3]$, the absorbance values increased with increasing $[\text{HNO}_3]$, but the dependence was less at the lower $[\text{HNO}_3]$. The list of the reaction conditions and the kinetic measurements are summarized in Table 5.

Table 3. Absorbance values at 350nm for $\text{Ce}(\text{NO}_3)_4$ Solutions

Abs. [HNO_3],M	[$\text{Ce}(\text{NO}_3)_4$], mM					Slope	R^2
	0.10	0.20	0.40	0.60	0.80		
0.20	0.0333	0.0667	0.1333	0.2000	0.2667	333.3	1.0
0.50	0.0833	0.1667	0.3333	0.5000	0.6667	833.3	1.0
1.00	0.1538	0.3077	0.6154	0.9231	1.2308	1538.5	1.0
2.00	0.3030	0.6061	1.2121	1.8182	2.4242	3030.3	1.0

Table 4. Absorbance values at 350nm for $\text{Ce}(\text{NO}_3)_3$ Solutions

Abs. [HNO_3],M	[$\text{Ce}(\text{NO}_3)_3$], mM					Slope	R^2
	0.10	0.20	0.40	0.60	0.80		
0.20	0.0009	0.0018	0.0360	0.0055	0.0073	9.1	1.0
0.50	0.0021	0.0042	0.0083	0.0125	0.0167	20.8	1.0
1.00	0.0040	0.0080	0.0160	0.0240	0.0320	40.0	1.0
2.00	0.0077	0.0154	0.0308	0.0462	0.0615	76.9	1.0

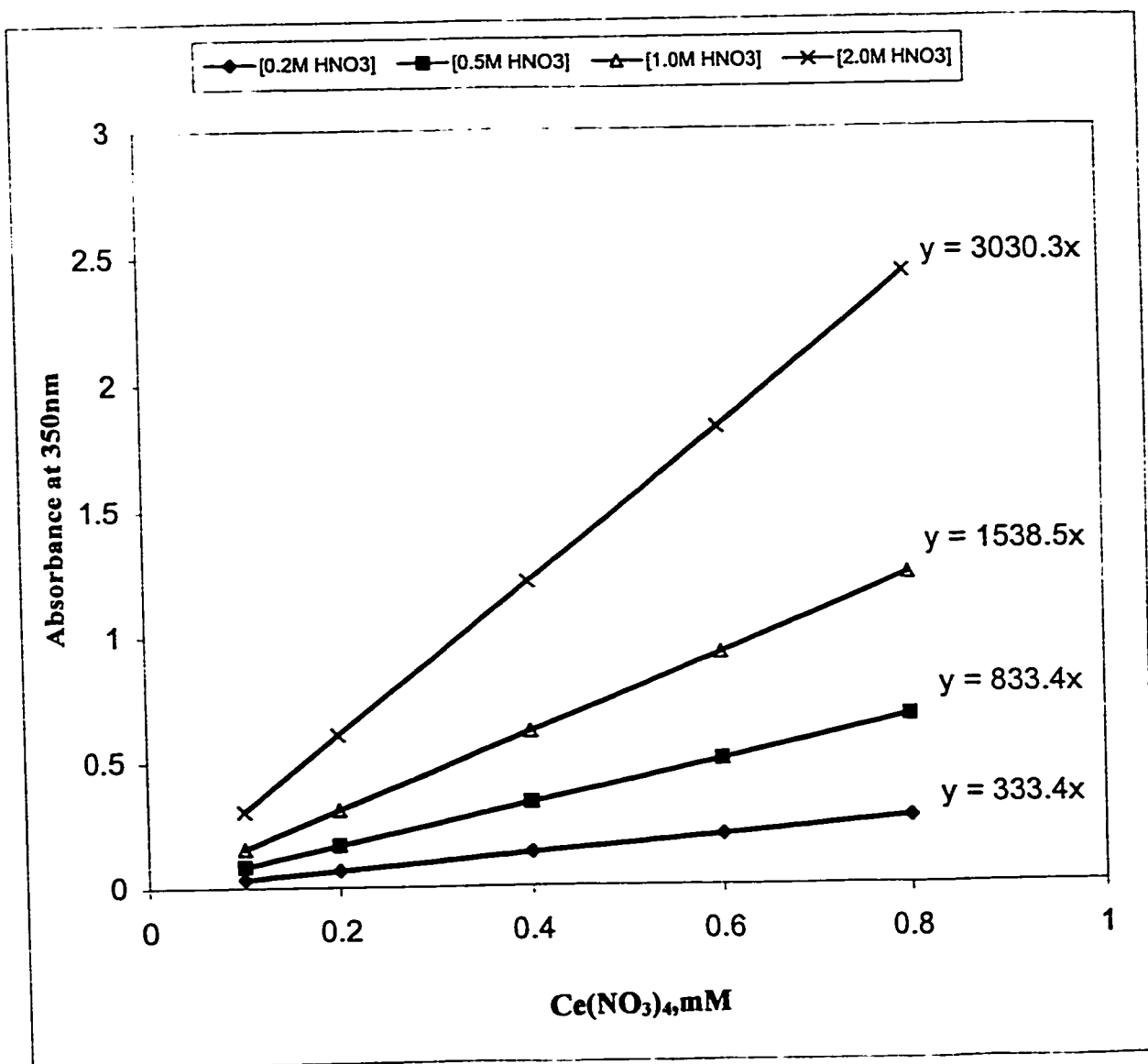


Figure 7. Absorbance of $\text{Ce}(\text{NO}_3)_4$ at 350nm with different $[\text{HNO}_3]$.

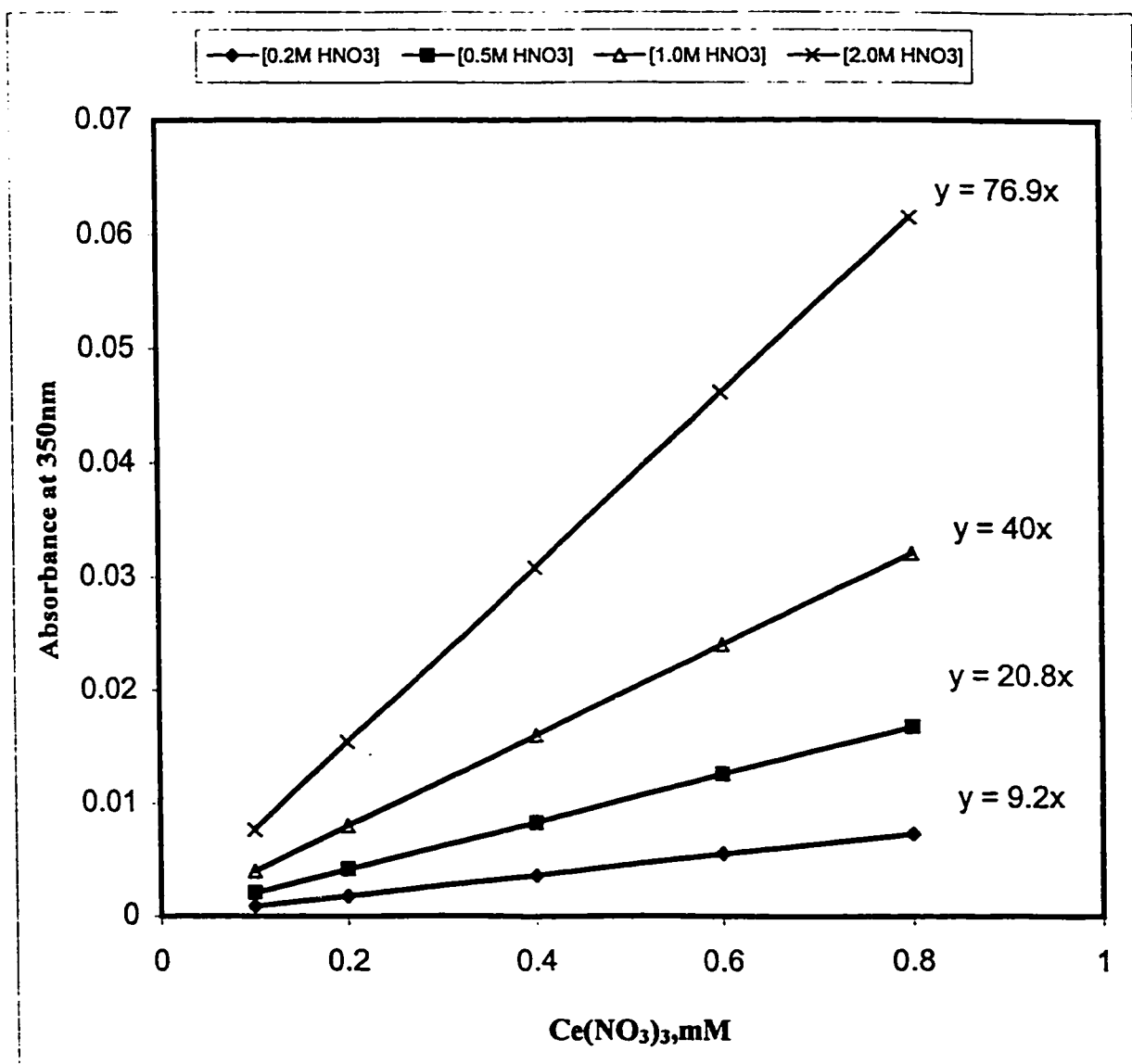


Figure 8. Absorbance of $\text{Ce}(\text{NO}_3)_3$ at 350nm with different $[\text{HNO}_3]$.

Table 5. Summary of Reaction Rate Constants

Temperature = 20°C									
Run	[Ce(NO ₃) ₄], mM	[EG], mM	[HNO ₃], M	(Abs.) ₀	k', min ⁻¹	k'x10 ⁴ , s ⁻¹	t _{1/2} , min	k ₂ , l/(mol.s)	Method
1	0.10	1.5	2.0	0.2989	0.0108	1.800	64	0.1200	Aliq.
2	0.10	1.5	2.0	0.2973	0.0101	1.683	69	0.1122	Aliq.
3	0.10	1.5	2.0	0.2965	0.0097	1.617	71	0.1078	Aliq.
4	0.20	1.5	2.0	0.5869	0.0105	1.750	66	0.1167	Aliq.
5	0.20	1.5	2.0	0.5873	0.0103	1.717	67	0.1144	Aliq.
6	0.10	3.0	2.0	0.2961	0.0212	3.533	33	0.1178	Aliq.
7	0.10	3.0	2.0	0.2953	0.0212	3.533	33	0.1178	Sing.
8	0.10	1.5	1.0	0.1487	0.0202	3.367	34	0.2244	Aliq.
9	0.10	1.5	1.0	0.1491	0.0203	3.383	34	0.2256	Sing.
10	0.20	1.5	1.0	0.2964	0.0210	3.500	33	0.2333	Aliq.
11	0.20	1.5	1.0	0.2958	0.0212	3.533	33	0.2356	Sing.
12	0.40	1.5	1.0	0.6053	0.0209	3.483	33	0.2322	Aliq.
13	0.40	1.5	1.0	0.6048	0.0212	3.533	33	0.2356	Sing.
14	0.50	1.5	1.0	0.7594	0.0208	3.467	33	0.2311	Aliq.
15	0.50	1.5	1.0	0.7588	0.0212	3.533	33	0.2356	Sing.
16	0.10	3.0	1.0	0.1452	0.0396	6.600	18	0.2200	Aliq.
17	0.10	3.0	1.0	0.1458	0.0398	6.633	17	0.2211	Sing.
18	0.10	4.5	1.0	0.1429	0.0611	10.183	11	0.2263	Sing.

Table 5. Summary of Reaction Rate Constants (Cont'd)

Temperature = 20°C									
Run	[Ce(NO ₃) ₄], mM	[EG], mM	[HNO ₃], M	(Abs.) ₀	k', min ⁻¹	k'x10 ⁴ , s ⁻¹	t _{1/2} , min	k ₂ , l/(mol.s)	Method
19	0.10	4.5	1.0	0.1432	0.0614	10.233	11	0.2274	Sing.
20	0.10	6.0	1.0	0.1391	0.0803	13.383	9	0.2231	Sing.
21	0.10	6.0	1.0	0.1389	0.0804	13.400	9	0.2233	Sing.
22	0.10	1.5	0.5	0.0769	0.0359	5.983	19	0.3989	Sing.
23	0.10	1.5	0.5	0.0762	0.0367	6.117	19	0.4078	Sing.
24	0.10	1.5	0.2	0.0301	0.0635	10.583	11	0.7056	Sing.
25	0.10	1.5	0.2	0.0304	0.0637	10.617	11	0.7078	Sing.
26	0.40	0.8	1.0	0.0610				0.3238	Aliq.
Temperature = 40°C									
Run	[Ce(NO ₃) ₄], mM	[EG], mM	[HNO ₃], M	(Abs.) ₀	k', min ⁻¹	k'x10 ⁴ , s ⁻¹	t _{1/2} , min	k ₂ , l/(mol.s)	Method
27	0.10	1.5	2.0	0.2601	0.0321	5.350	22	0.3567	Aliq.
28	0.10	1.5	2.0	0.2589	0.0324	5.400	22	0.3600	Aliq.
Temperature = 60°C									
Run	[Ce(NO ₃) ₄], mM	[EG], mM	[HNO ₃], M	(Abs.) ₀	k', min ⁻¹	k'x10 ⁴ , s ⁻¹	t _{1/2} , min	k ₂ , l/(mol.s)	Method
29	0.10	1.5	2.0	0.2096	0.0776	12.933	9	0.8622	Aliq.
30	0.10	1.5	2.0	0.2091	0.0777	12.950	9	0.8633	Aliq.

Note: The concentration values here indicate the reaction solutions.

Inspection of the data for the kinetic measurements at 20°C reveals that the two sampling methods yield the same result with excellent agreement as expected. Therefore, the volume change in the reactor solutions during the reaction process does not affect the reaction rate. Typical measurements of each method are shown in Figures 9 and 10 for the reaction solutions containing 0.1mM Ce(NO₃)₄ / 1.0M HNO₃ and 1.5mM EG. The corresponding data are listed in Appendix A and B. The decrease in absorbance with time was fit to a first-order rate expression with R² = 0.9997-0.9999. The rate expressions are,

$$\ln(1/(1-X)) = 0.0202 t + 0.0119, \text{ (Aliquot method)}$$

and $\ln(1/(1-X)) = 0.0203 t + 0.0116. \text{ (Single sample method)}$

For these conditions, the calculated k's were 0.0202 min⁻¹ (Aliquot method) and 0.0203 min⁻¹ (Single sample method). The k's from these two methods agreed within 99.75%. Therefore, the aliquot method can be used conveniently and confidently in the higher temperature measurements.

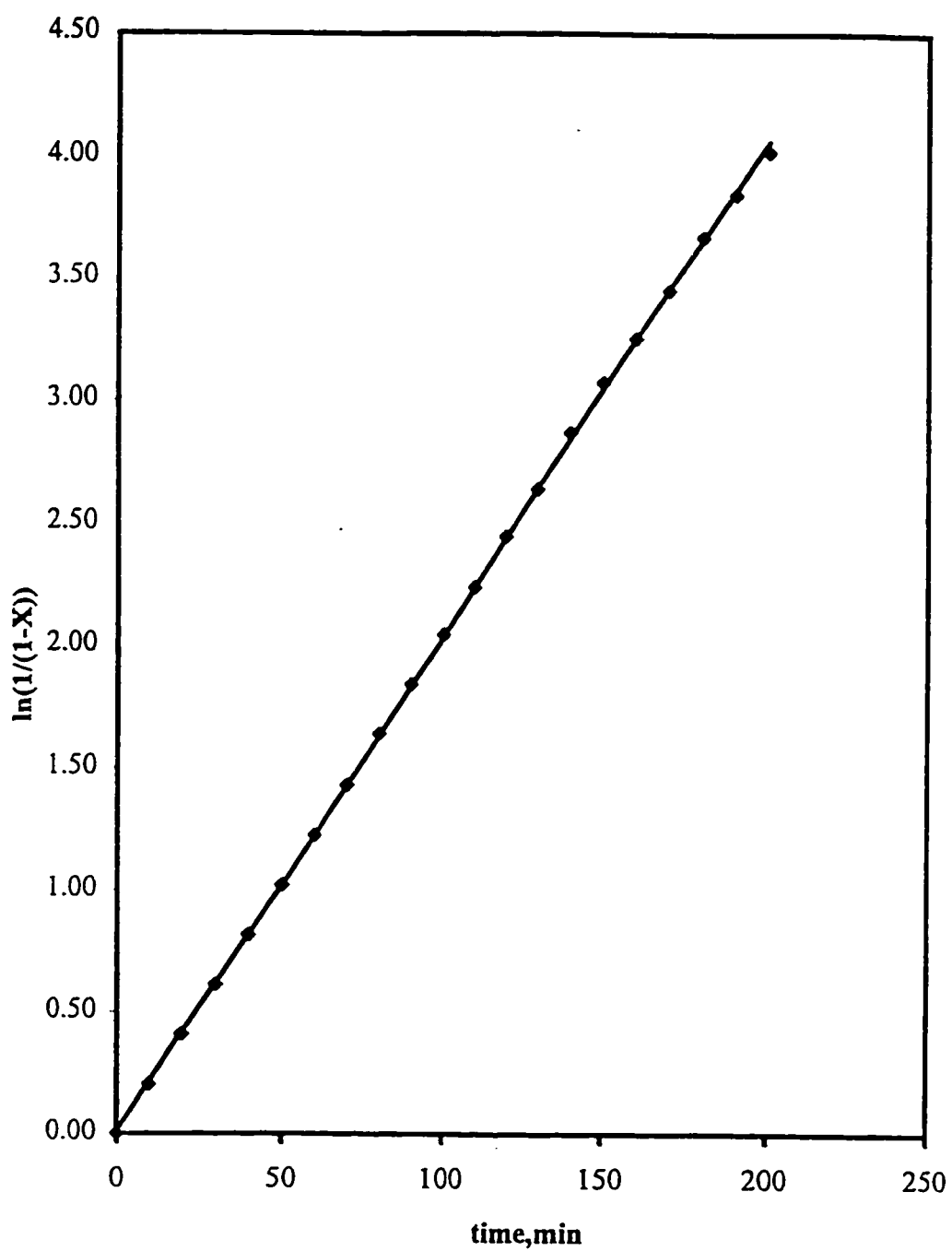


Figure 9. Plot of $\ln(1/(1-X))$ versus time (Aliquot method).

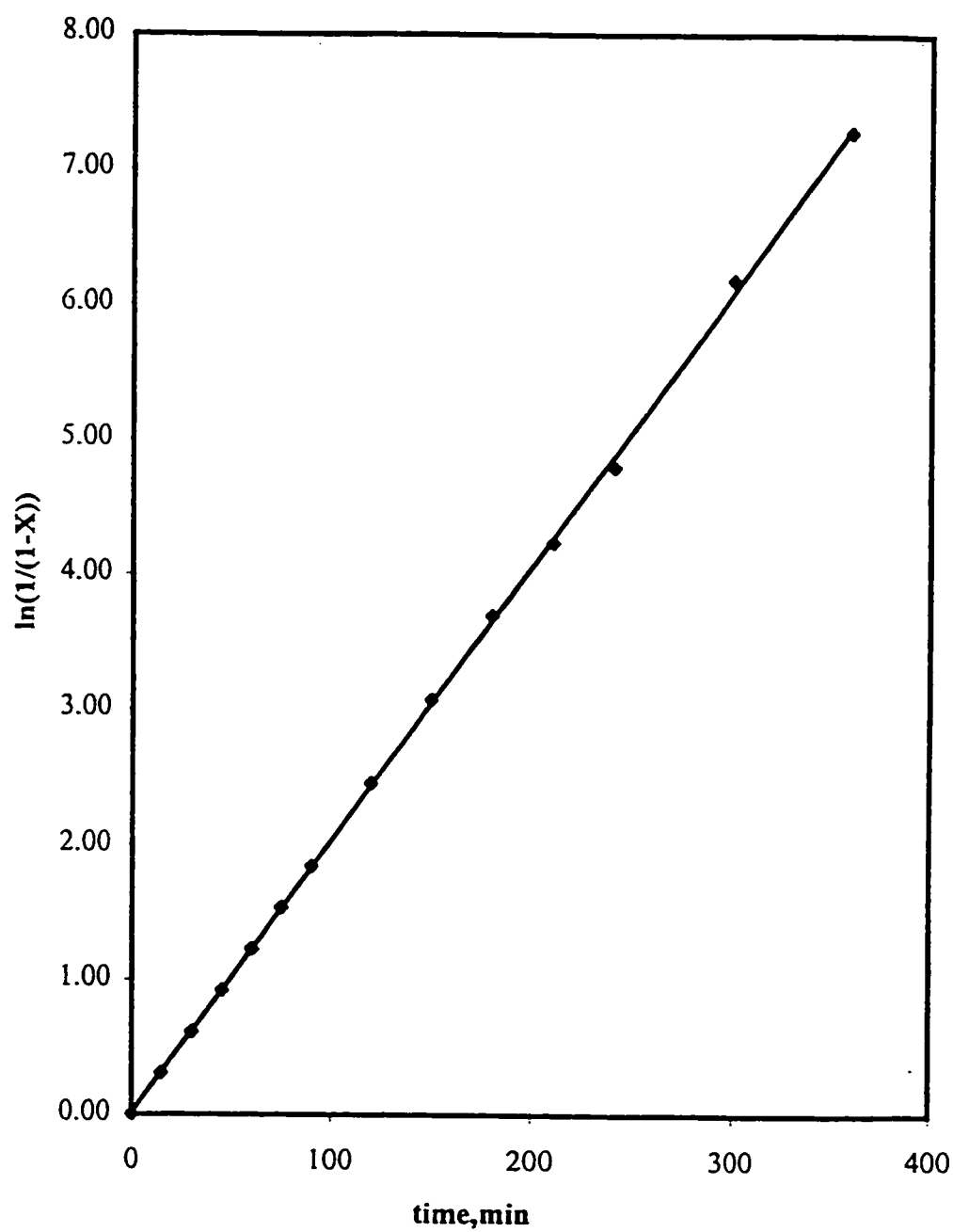


Figure 10. Plot of $\ln(1/(1-X))$ versus time (Single sample method).

The fit of the data to the first order rate law and the fact that the k' values are independent of the initial $[\text{Ce}(\text{NO}_3)_4]$ demonstrate that the reaction is first order in $[\text{Ce}(\text{NO}_3)_4]$. The average k' value is $(3.48 \pm 0.10) \times 10^{-4} \text{ s}^{-1}$ with $<3\%$ error and k_2 value is $(0.231 \pm 0.006) \text{ L}/(\text{mol}\cdot\text{s})$ in 1.0M HNO_3 at 20°C . The data for the reaction conditions with excess 1.5mM EG in 1.0M HNO_3 at 20°C are collected in Table 6. The constancy of k' with varying $[\text{Ce}(\text{IV})]$ for the reaction conditions with a large excess of PEG in the $0.05\text{M H}_2\text{SO}_4$ medium at 26°C was reported by Nagarajan et al. [5]. They reported an average k' value of $(1.39 \pm 0.072) \times 10^{-4} \text{ s}^{-1}$ with $<5\%$ error and k_2 value was $(0.046 \pm 0.002) \text{ L}/(\text{mol}\cdot\text{s})$ in $0.05\text{M H}_2\text{SO}_4$ at 26°C . Their rate constant is lower than this study. The differences may due to the two different reaction conditions: one used 1.5mM EG in 1.0M HNO_3 at 20°C and the other used 3mM PEG in $0.05\text{M H}_2\text{SO}_4$ at 26°C . However, the fact that the reaction was first order in $[\text{Ce}(\text{NO}_3)_4]$ agreed with their study.

Table 6. Effect of $[\text{Ce}(\text{NO}_3)_4]$ on the pseudo-first order rate constant
For conditions with excess 1.5mM EG in 1.0M HNO_3 at 20°C

$[\text{Ce}(\text{NO}_3)_4], \text{mM}$	(Abs.) _o	$k' \times 10^4, \text{s}^{-1}$	$t_{1/2}, \text{min}$	$k_2, \text{L} / (\text{mol}\cdot\text{s})$
0.10	0.1489	3.375	34	0.225
0.20	0.2961	3.517	33	0.234
0.40	0.6051	3.508	33	0.234
0.50	0.7591	3.500	33	0.233
Ave:		3.48 ± 0.10		0.231 ± 0.006

The effect of [EG] on the oxidation reaction rate was determined using solutions containing 0.2mM Ce(NO₃)₄ / 2.0M HNO₃ at 20°C and varying amounts of excess EG. It was found that the pseudo-first-order rate constants increased with the increase of [EG], however, the calculated second-order rate constants remained constant. These data are listed in Table 7. The average k₂ value is: (0.224±0.003) L/(mol*s) in 1.0M HNO₃ at 20°C.

Table 7. Effect of [EG] on the pseudo-first order rate constant
For conditions with 0.1mM Ce(NO₃)₄ in 1.0M HNO₃ at 20°C

[EG],mM	(Abs.) _o	k' x 10 ⁴ , s ⁻¹	t _{1/2} , min	K ₂ , L / (mol*s)
1.5	0.1489	3.375	34	0.225
3.0	0.1455	6.617	17	0.221
4.5	0.1431	10.208	11	0.227
6.0	0.1390	13.392	9	0.223
Ave:				0.224 ± 0.003

The reaction order (n) with respect to [EG] was determined using the relationship,

$$k' = k_2 * [EG]^n$$

As seen in Figure 11, the plot of log k' against log [EG] using the data from Table 7 produced a straight line with a slope of unity. The data is fit by the following equation,

$$\log k' = 1.0007 \log [EG] + 0.3488, \quad R^2 = 0.9999$$

Thus, the reaction is first-order in [EG] and the overall order of this reaction is two at constant [HNO₃].

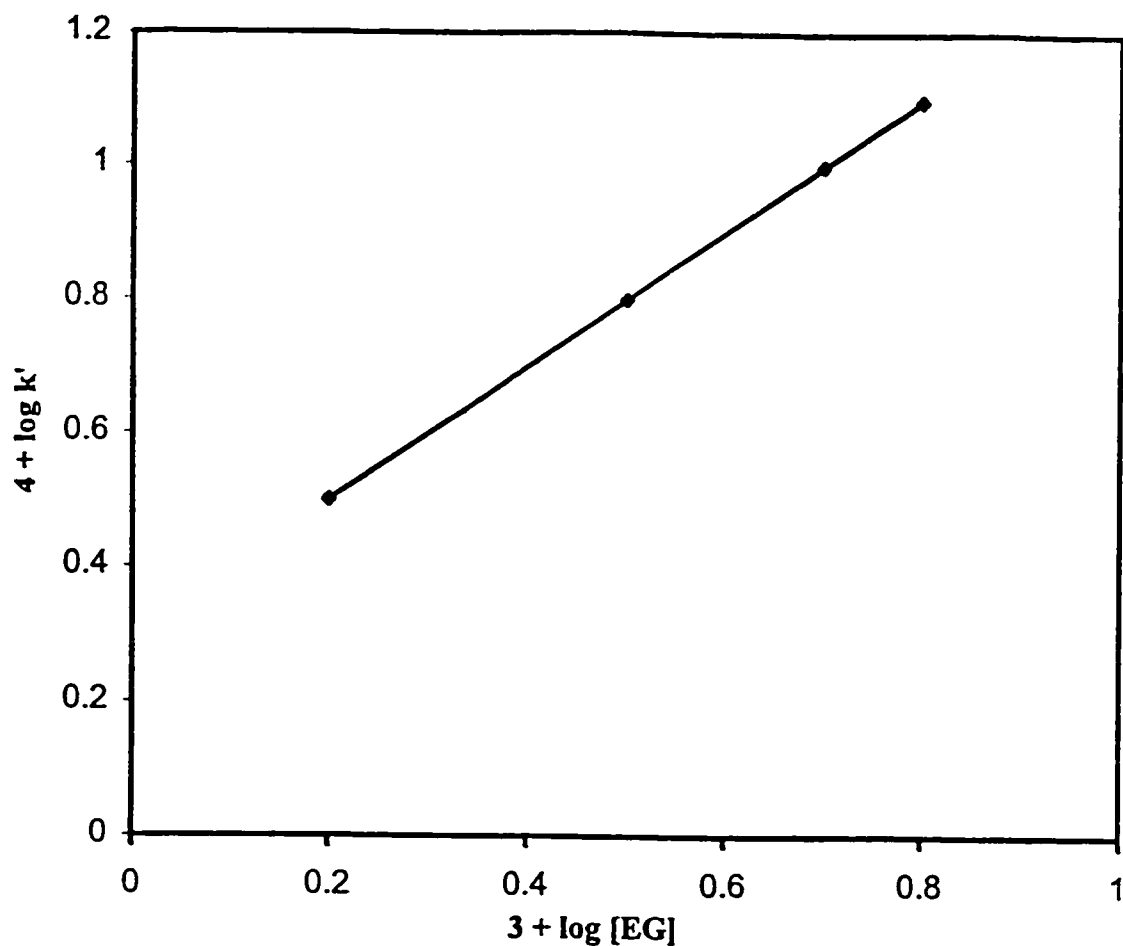


Figure 11. Plot of $\log k'$ against $\log [\text{EG}]$.

Nagarajan et al. [5] reported that the H_2SO_4 had a strong effect on the reaction rate when the ionic strength was not constant. In our study, the reaction rates were measured in the solutions containing 0.2-2.0 M HNO_3 , 0.1mM $\text{Ce}(\text{NO}_3)_4$ and 1.5mM EG at 20°C.

As seen in Table 8, the pseudo-first-order rate constants decreased directly with the increase in the $[\text{HNO}_3]$. The plot of $\log k'$ against $\log [\text{HNO}_3]$ is shown in Figure 12 and reveals that the relationship is not linear over all of the concentration range. The dependency seems to be linear at $[\text{HNO}_3]$ greater than 0.5M. In this concentration range, the reaction appears to have a -1 order with respect to $[\text{HNO}_3]$. Hence the kinetic expression can be written as,

$$\text{Rate} = k_2 [\text{Ce}(\text{NO}_3)_4] [\text{EG}]/[\text{HNO}_3] \quad (\text{for } [\text{HNO}_3] > 0.5\text{M}) \quad (31)$$

This expression is consistent with Nagarajan's study [5], where

$$\text{Rate} = K'[\text{Ce(IV)}][\text{PEG}] / [\text{H}_2\text{SO}_4] \quad (8)$$

Table 8. Effect of $[\text{HNO}_3]$ on the pseudo-first order rate constant for conditions with 0.1mM $\text{Ce}(\text{NO}_3)_4$ and 1.5mM EG at 20°C

$[\text{HNO}_3]$, M	(Abs.) _o	$k' \times 10^4$, s ⁻¹	$t_{1/2}$, min	k_2 , L / (mol*s)
2.0	0.2976	1.700	68	0.113
1.0	0.1489	3.375	34	0.225
0.5	0.0766	6.050	19	0.403
0.2	0.0303	10.600	11	0.707

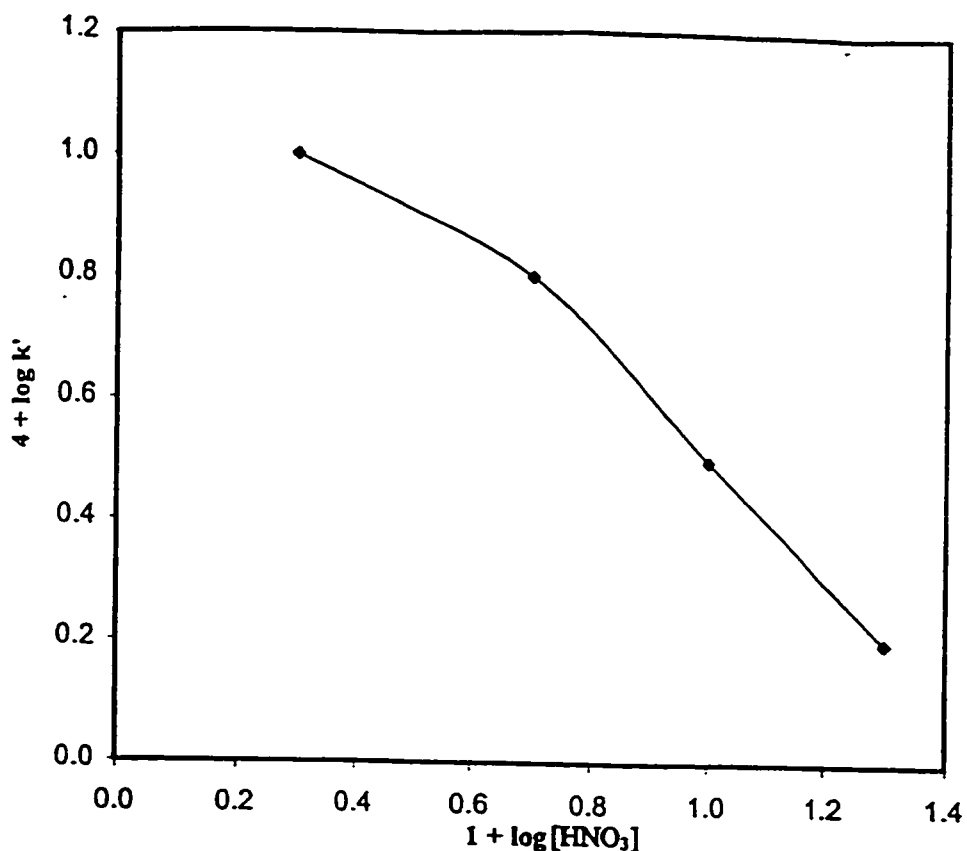


Figure 12. Plot of $\log k'$ against $\log [\text{HNO}_3]$.

To verify the overall reaction order, one measurement was made at 20°C using nearly equal concentrations of $\text{Ce}(\text{NO}_3)_4$ and EG. The reaction solution contained 0.4mM $\text{Ce}(\text{NO}_3)_4$ / 1.0M HNO_3 and 0.75mM EG where $[\text{EG}]:[\text{Ce}(\text{NO}_3)_4] = 1.9$, and the change in the $\text{Ce}(\text{NO}_3)_4$ absorbance was treated using Equation 18. The data are listed in Appendix C and the plot of $\ln [a(b-x)/b(a-x)]$ against time is shown in Figure 13 and the data is fit by the following equation,

$$\ln[a(b-x)/b(a-x)] = 0.0068 t + 0.0153, \quad R^2 = 0.9999 \quad (32)$$

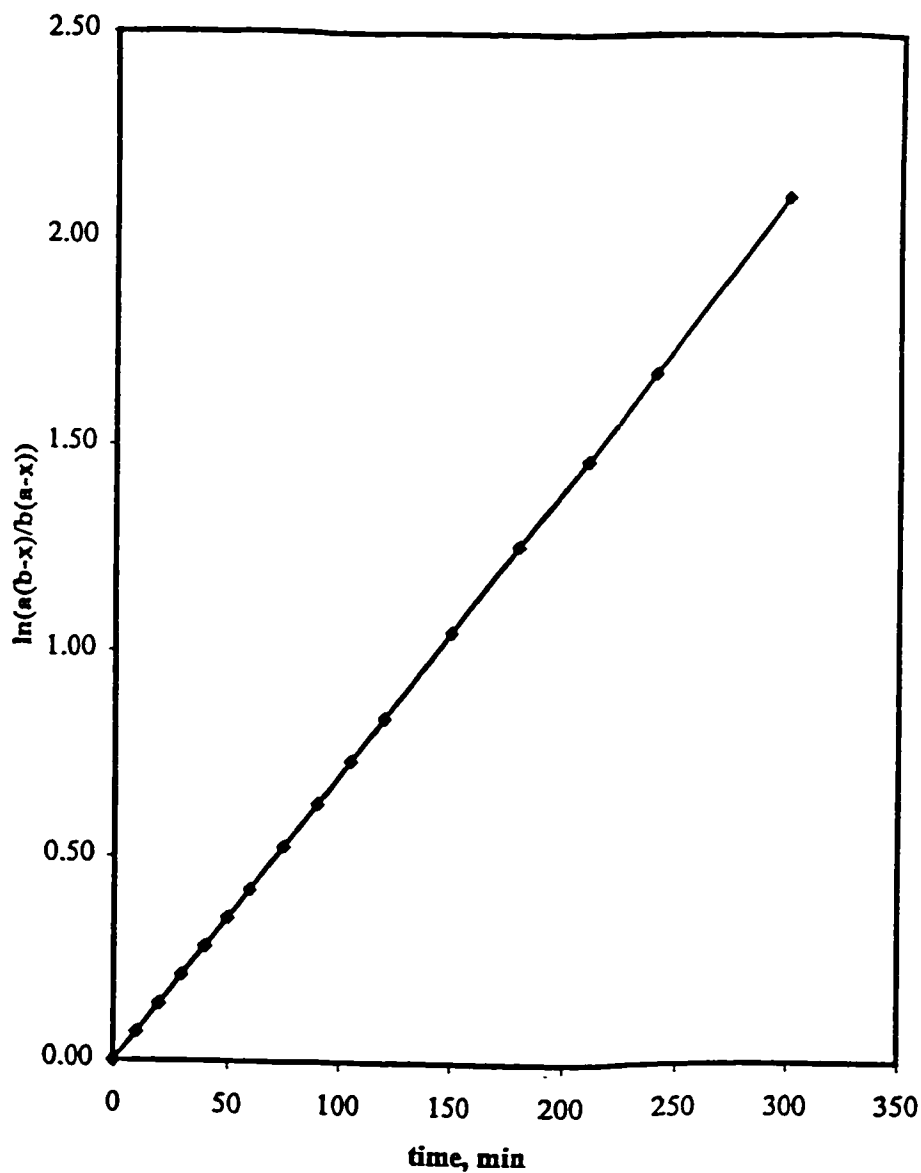


Figure 13. Plot of $\ln(a(b-x)/b(a-x))$ against time.

The fit of the points to this line is very good and suggests that the reaction is second-order even though the stoichiometry for the complete reaction is 10:1. From the slope

value of 0.0068min^{-1} , the k_2 value is estimated equal to $0.324\text{ L}/(\text{mol}\cdot\text{s})$ obtained in 1.0M HNO_3 at 20°C and using $0.0068 / (0.00075-0.0004)$ from Equation 18. The k_2 value obtained by the second-order method is 30-50% higher than the value ($0.231\text{ L}/\text{mol}\cdot\text{s}$) in 1.0M HNO_3 at 20°C obtained by the pseudo-first-order method. This difference may reflect an error in using the second-order kinetic expression with the sampling procedure since at the practical initial time ($t = 0$) there may already be some reaction. Thus, the $(b-a)$ term in Equation 18 should not be $(0.00075-0.0004)$. The actual value of the $(b-a)$ term will be larger and is expected to provide a smaller k_2 value than the one calculated using the initial concentrations.

If the stoichiometry of the overall reaction ($10\text{ Ce}(\text{NO}_3)_4 : 1\text{ EG}$) is considered in the rate expressions, Equation 18 becomes,

$$k_2 t = \{1/(0.1[\text{Ce}(\text{NO}_3)_4]_0 - [\text{EG}]_0)\} \ln\{[\text{EG}]_0[\text{Ce}(\text{NO}_3)_4]_t / [\text{Ce}(\text{NO}_3)_4]_0[\text{EG}]_t\}$$

or $k_2 t = \{1/(0.1a-b)\} \ln\{b(a-x) / a(b-0.1x)\}$

The data are listed in Appendix D and the plot of $\ln[a(b-0.1x)/b(a-x)]$ against time is shown in Figure 14. As can be seen, the plot is not linear. When a stoichiometry relationship ($2\text{Ce}(\text{NO}_3)_4 : 1\text{ EG}$) is used, Equation 18 becomes,

$$k_2 t = \{1/(0.5[\text{Ce}(\text{NO}_3)_4]_0 - [\text{EG}]_0)\} \ln\{[\text{EG}]_0[\text{Ce}(\text{NO}_3)_4]_t / [\text{Ce}(\text{NO}_3)_4]_0[\text{EG}]_t\}$$

or $k_2 t = \{1/(0.5a-b)\} \ln\{b(a-x) / a(b-0.5x)\}$

The plot of $\ln[a(b-0.5x)/b(a-x)]$ against time is still not linear. This plot is shown in Appendix E. Therefore, the lack of linearity indicates that the overall stoichiometry of the reaction is not important in the kinetic reaction. Also, this is a reaction involving many

steps, but the slow step has a composition which includes one molecular of $\text{Ce}(\text{NO}_3)_4$ and one molecular of EG.

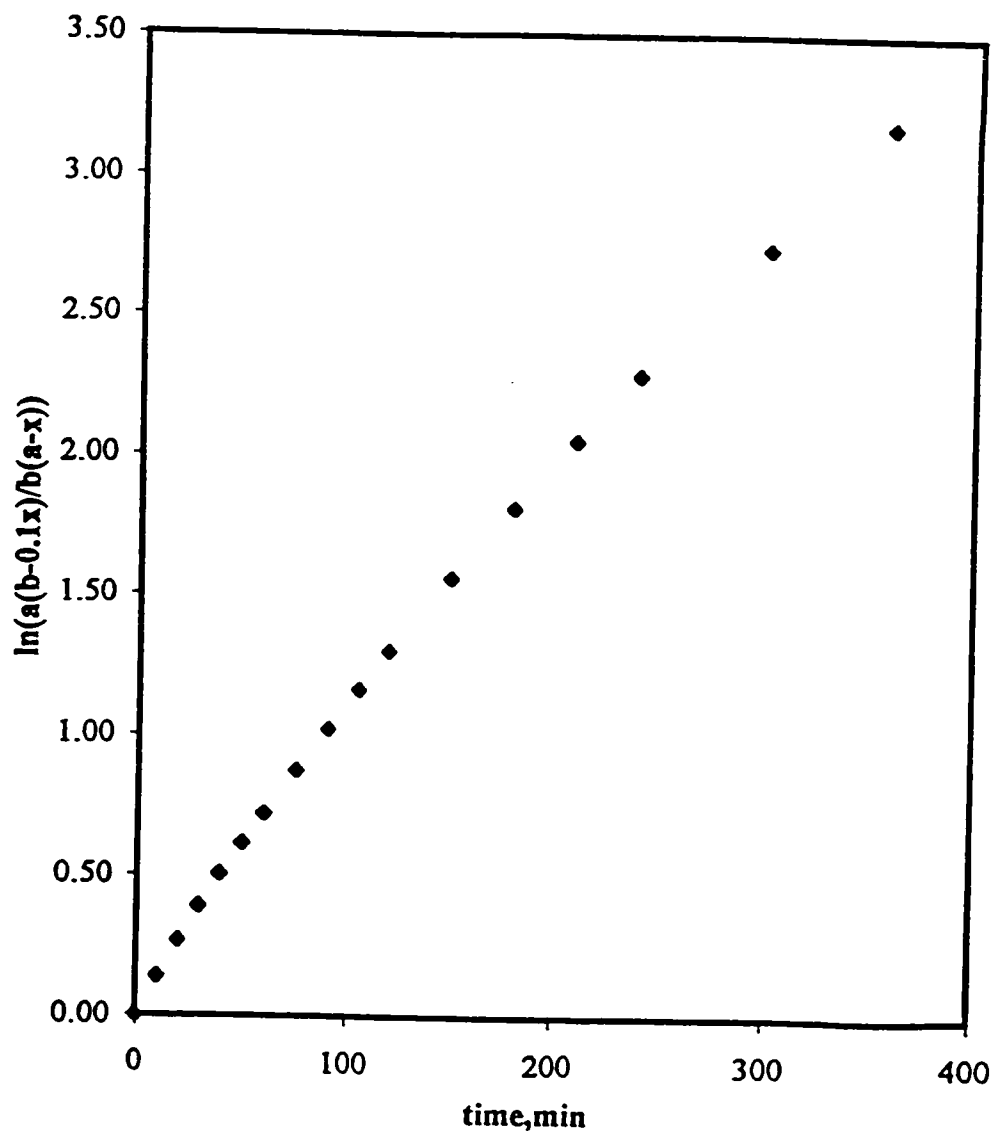


Figure 14. Plot of $\ln(a(b-x)/b(a-0.1x))$ against time.

Effect of Temperature

Using the same reaction solutions which contain 0.1mM Ce(NO₃)₄ / 2.0M HNO₃ and 1.5mM EG, the reaction rates were measured at 20°C, 40°C and 60°C. The rate measurements were run twice at each temperature to confirm the reproducibility. The aliquot method was used and the decrease in Ce(NO₃)₄ absorbance with time was fit to the corresponding first-order rate law. The plots always produced good straight lines with R²= 0.9990-0.9996. The calculated average k's values were 0.0102min⁻¹, 0.0323min⁻¹ and 0.0777min⁻¹ and the k₂ values were 6.8 L/(mol*s), 21.5 L/(mol*s) and 51.8 L/(mol*s) in 2.0 M HNO₃ at 20°C, 40°C and 60°C, respectively.

The plot of ln k₂ against 1/T is shown in Figure 15 and the data is fit the following equation,

$$\ln k_2 = -5026 \times (1/T) + 19.2, \quad R^2 = 0.9947 \quad (33)$$

Thus, the second-order rate constants increased with increasing temperature. This indicates that the reaction is an activated reaction and obeys the Arrhenius Equation. From Equation 33, the activation energy was calculated to be 9.99 Kcal/mol.

The transition state parameters ΔH*, ΔG* (20 °C) and ΔS* were calculated to be 9.41Kcal/mol, 22.21Kcal/mol and -43.68 Cal/(mol*K) from Equations 24-26. These data were tabulated in Table 9 and compared with the data reported by Nagarajan et al. [5]. As can be seen, the values from both studies are in close agreement even though the molecular weight of the EG derivatives are very different. Thus, the thermodynamic parameters seem to be independent of the molecular weight of the EG derivatives.

Similar calculations were made using the pseudo-first-order rate constants (k') and the corresponding data are also presented in Table 9.

Table 9. Comparison of the thermodynamic parameters

Organics	This study		Reference [5]		
	EG(k')	EG(k_2)	PEG 400	PEG 4000	PEG 6000
Ea, Kcal/mol	9.99	9.99	10.49	9.81	8.58
ΔG^\ddagger , Kcal/mol	22.21	18.02	24.07	21.84	20.45
ΔH^\ddagger , Kcal/mol	9.41	9.41	9.86	9.22	8.00
ΔS^\ddagger , Cal/(mol*K)	-43.68	-39.36	-47.22	-43.04	-42.50

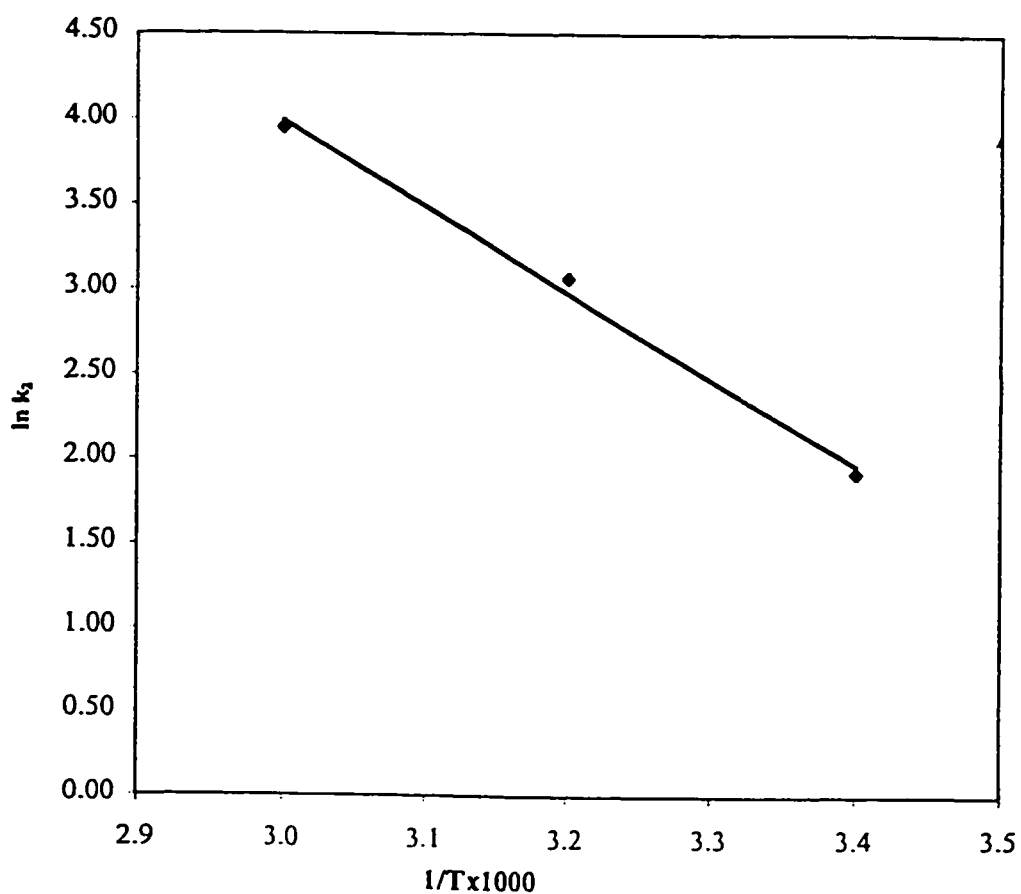


Figure 15. Plot of $\ln k_2$ against $1/T$

In considering a practical wastewater clean-up process, there is a need to determine the reaction time for complete consumption of the organic contaminants in order to select the flow rate of the process. Consider a reactor operating at 100°C and containing 10mM $\text{Ce}(\text{NO}_3)_4$ / 2.0M HNO_3 and 1.5mM EG, where $[\text{Ce}(\text{NO}_3)_4] \gg [\text{EG}]$. The second-order rate constant is calculated to be 306.6 L/(mol*s) in 2.0 M HNO_3 at 100°C, the corresponding pseudo-first-order rate constant (k') would be 3.1 s⁻¹ and the reaction half-life would be approximate 0.3 second. For this case, the complete reaction (99.99%) of the organic contaminant would occur within 3 seconds. With a reactor size of one gallon, a flow rate of up to 20 gals/min could be used and still remove the organic contaminant by this process. (Other considerations aside.)

Comparison with the report by Nagarajan et al. [5]

In the Nagarajan et al. paper [5], the absorbance at 304nm was used for their kinetic measurements. We found that it was hard to determine accurately the $\text{Ce}(\text{NO}_3)_4$ and $\text{Ce}(\text{NO}_3)_3$ absorbances at 304nm because the absorption spectra were not stable at this wavelength. We selected 350nm as the analytical wavelength for our kinetic study. The authors reported that the oxidation reaction of PEG by Ce(IV) in H_2SO_4 medium was a second-order reaction, first-order in each reactant. Also, they reported that the k' value was independent of the $[\text{Ce}(\text{IV})]$. These conclusions were verified in this study. We found the oxidation reaction of EG by $\text{Ce}(\text{NO}_3)_4$ in HNO_3 solution was first-order in each reactant. However, we measured the higher rate constants than they reported. The effect of acid concentration on the reaction rate was also confirmed, i.e., the reaction rate constant decreased with an increase in the acid concentration when the ionic strength was not a constant. We agree on the form of the overall reaction kinetic expressions, as shown in Equations 8 and 31, and on the values of the thermodynamic parameters. However, the authors did not provide the data and equations used to calculate the thermodynamic parameters. This agreement indicates that the thermodynamic parameters seem to be independent of the molecular weight of the EG derivatives.

Chapter VI

Conclusions

The kinetics of oxidation reaction of EG by $\text{Ce}(\text{NO}_3)_4$ in aqueous HNO_3 solution was studied at 20°C, 40°C and 60°C. This reaction is a part of the overall MEO process and EG was selected as the prototype organic compound. This reaction was studied by measuring the change in the optical absorption at 350nm using an UV-Vis spectrophotometer. The reaction was found to be first order with respect to $\text{Ce}(\text{NO}_3)_4$ and EG and -1 order with respect to HNO_3 (for the condition $[\text{HNO}_3] > 0.5\text{M}$). The pseudo-first-order approximation method was used where the $[\text{EG}]$ was in large excess to the $[\text{Ce}(\text{NO}_3)_4]$. The second-order rate constant was determined to be $0.228 [\text{HNO}_3] \text{ L}/(\text{mol}\cdot\text{s})$ at 20°C. Good pseudo-first-order rate constants were also obtained at 40°C and 60°C. The reaction rates were faster at these temperatures, as expected for an activated reaction. From the fit of the rate constant values to the Arrhenius Equation, E_a , ΔH^* , ΔG^* (20°C) and ΔS^* were calculated equal to 10.0 Kcal/mol, 9.4Kcal/mol, 22.2Kcal/mol and $-43.7\text{Cal}/(\text{mol}\cdot\text{K})$, respectively. These values compared well with those reported in the literature with PEG. Thus, the reaction kinetics seems to be independent of the molecular weight of the EG derivatives.

Chapter VII

Suggestions for Further Study

1. The HPLC technique can also be used to corroborate the decrease in [EG] using the following expression which relates area to [EG]: $A = f_w W = f_w u c M$
where A = peak area, f_w = correlation factor, W = the mass of entering sample,
 u = the flow rate of carrier gas, M = the molecular weight of EG, and c = [EG].
The linearity of A - [EG] relationship can be determined first, and Equation 18 can be written in terms of the area and used to determine k'' value using
 $\ln (A_0 / A_t) = k'' t$.
2. The mechanism of the reaction needs further study.
3. Wastewater containing chlorinated compounds, halogenated compounds and non-soluble compounds should be tested to determine the effectiveness of the Ce(IV) oxidation process.

REFERENCES

- [1]. Barnes, D., Bliss, P. J., Gould, B. W. and Vallentine, H. R., Water and Wastewater Engineering System, Pitman, (1981), pp.148-150.
- [2]. Jorgensen, S.E., Industrial Waste Water Management, Elsevier Science, (1979), pp. 153-160.
- [3]. Culp, R.L., Wesner, G.M. and Culp, G.L., Handbook of Advanced Wastewater Treatment, Van Nostrand Reinhold, (1978), pp. 249-294.
- [4]. J.Bringmann, K.Ebert, U.Galla and H.Schmieder, "Electrochemical mediators for total oxidation of chlorinated hydrocarbons: formation kinetics of Ag(II), Co(III), and Ce(IV)", Journal of Applied Electrochemistry, Vol.25, 1995, pp.846-851.
- [5]. S. Nagarajan, K.S.V. Srinivasan, and K.Venkata Rao, "Kinetic and Mechanistic Studies on the Oxidation of Poly(ethylene glycol) by Ceric Sulphate in Sulphuric Acid Medium", Polymer Journal, Vol. 26, No.7, 1994, pp.851-857.
- [6]. Laidler, K.J. and Meiser, J.H., Physical Chemistry, Benjamin and Cummings, (1982), pp.353-357.
- [7]. Joseph C. Farmer, Francis T. Wang, Ruth A. Lewis, Leslie J. Summers and Linda Foiles, "Electrochemical Treatment of Mixed and Hazardous Wastes: Oxidation of Ethylene Glycol and Benzene by Silver(II)", Journal of Electrochemical Society, Vol.139, No.3, March 1992, pp.654-661.
- [8]. Joseph C. Farmer, Francis T. Wang, Patricia R. Lewis and Leslie J. Summers, "Destruction of Chlorinated Organics by Cobalt (III)- Mediated Electrochemical Oxidation", Journal of Electrochemical Society, Vol.139, No.11, November 1992, pp. 3025-3029.
- [9]. J.M. Nzikou, M. Aurousseau, and F. Lapicque, "Electrochemical investigation of the Ce(III)/Ce(IV) couple related to a Ce(IV)-assisted process for SO₂/NO_x abatement", Journal of Applied Electrochemistry, Vol.25, 1995, pp.967-972.
- [10]. M. Aurousseau, C. Roizard, A. Storck, and F. Lapicque, "Scrubbing of Sulfur

- Dioxide Using a Cerium(IV)- Containing Acidic Solution: A Kinetic Investigation", Industria & Engineering Chemistry Research, Vol.35, No.4, 1996, pp.243-1250.
- [11]. M. Aurousseau, F. Lapique, C. Francois, and A. Storck, "Simulation of Nox scrubbing by ceric solution: Oxidation of nitrous acid by Ce(IV) species in acidic solutions", Industrial & Engineering Chemistry Research, Vol.33, No.2, 1994, pp.191-196.
- [12]. V. S. Mishra, V. V. Mahajani, and J. B. Joshi, "Wet air oxidation", Industrial & Engineering Chemistry Research, Vol.34, No.1, 1995, pp.22-48.
- [13]. Moore, J. W. and Pearson, R. G., "Kinetics and Mechanism", John Wiley & Sons, 1981, pp.128-129.
- [14]. James, W.Cooper, "Spectroscopic Techniques for Organic Chemists", John Wiley & Sons, 1983, pp.38-39.
- [15]. H.C. Grinter and T.L. Threlfall, "UV-VIS Spectroscopy and Its Applications", Springer-Verlag, 1992, pp.3-10

APPENDIX A. Data provided for Figure 9

Time(min)	$\ln(1/(1-X))$	X	Abs.	Abs(IV)	[Ce(IV)]	Abs (III)	[Ce(III)]
0	0.00	0.0000	0.1487	0.1487	9.67E-05	0.0000	0.00E+00
10	0.20	0.1841	0.1221	0.1213	7.89E-05	0.0008	1.93E-05
20	0.41	0.3356	0.1002	0.0988	6.42E-05	0.0014	3.52E-05
30	0.61	0.4588	0.0824	0.0805	5.23E-05	0.0019	4.82E-05
40	0.82	0.5592	0.0679	0.0656	4.26E-05	0.0023	5.87E-05
50	1.02	0.6408	0.0561	0.0534	3.47E-05	0.0027	6.73E-05
60	1.23	0.7073	0.0465	0.0435	2.83E-05	0.0030	7.43E-05
70	1.43	0.7612	0.0387	0.0355	2.31E-05	0.0032	7.99E-05
80	1.64	0.8062	0.0322	0.0288	1.87E-05	0.0034	8.47E-05
90	1.84	0.8415	0.0271	0.0236	1.53E-05	0.0035	8.84E-05
100	2.04	0.8706	0.0229	0.0192	1.25E-05	0.0037	9.14E-05
110	2.24	0.8934	0.0196	0.0158	1.03E-05	0.0038	9.38E-05
120	2.45	0.9135	0.0167	0.0129	8.36E-06	0.0038	9.59E-05
130	2.64	0.9287	0.0145	0.0106	6.89E-06	0.0039	9.75E-05
140	2.87	0.9433	0.0124	0.0084	5.48E-06	0.0040	9.90E-05
150	3.07	0.9536	0.0109	0.0069	4.48E-06	0.0040	1.00E-04
160	3.25	0.9612	0.0098	0.0058	3.75E-06	0.0040	1.01E-04
170	3.45	0.9682	0.0088	0.0047	3.08E-06	0.0041	1.02E-04
180	3.66	0.9744	0.0079	0.0038	2.47E-06	0.0041	1.02E-04
190	3.84	0.9785	0.0073	0.0032	2.07E-06	0.0041	1.03E-04
200	4.02	0.9820	0.0068	0.0027	1.74E-06	0.0041	1.03E-04

APPENDIX B. Data provided for Figure 10

Time(min)	$\ln(1/(1-X))$	X	Abs.
0	0.00	0.0000	0.1491
15	0.31	0.2646	0.1107
30	0.62	0.4597	0.0824
45	0.92	0.6023	0.0617
60	1.23	0.7078	0.0464
75	1.54	0.7850	0.0352
90	1.85	0.8422	0.0269
120	2.46	0.9145	0.0164
150	3.08	0.9538	0.0107
180	3.70	0.9752	0.0076
210	4.24	0.9855	0.0061
240	4.80	0.9917	0.0052
300	6.18	0.9979	0.0043
360	7.28	0.9993	0.0041

APPENDIX C. Data provided for Figure 13

Time(min)	$\ln(a(b-x)/b(a-x))$	$(b-x)/(a-x)$	x	X	Abs.
0	0.00	1.8750	0.00000	0.0000	0.6103
10	0.07	2.0110	0.00005	0.1345	0.5303
20	0.14	2.1568	0.00010	0.2436	0.4653
30	0.21	2.3131	0.00013	0.3337	0.4117
40	0.28	2.4809	0.00016	0.4091	0.3668
50	0.35	2.6608	0.00019	0.4731	0.3287
60	0.42	2.8537	0.00021	0.5280	0.2961
75	0.53	3.1696	0.00024	0.5967	0.2551
90	0.63	3.5205	0.00026	0.6528	0.2217
105	0.74	3.9103	0.00028	0.6993	0.1941
120	0.84	4.3432	0.00030	0.7383	0.1709
150	1.05	5.3581	0.00032	0.7992	0.1346
180	1.26	6.6102	0.00034	0.8440	0.1079
210	1.47	8.1548	0.00035	0.8777	0.0879
240	1.68	10.0604	0.00036	0.9034	0.0726
300	2.10	15.3116	0.00038	0.9389	0.0515

APPENDIX D. Data provided for Figure 14

Time(min)	$\ln(a(b-0.1x)/b(a-x))$	$(b-0.1x)/(a-x)$	x	X	Abs.
0	0.00	1.8750	0.00000	0.0000	0.6103
10	0.14	2.1510	0.00005	0.1346	0.5302
20	0.27	2.4467	0.00010	0.2436	0.4653
30	0.39	2.7638	0.00013	0.3337	0.4117
40	0.50	3.1039	0.00016	0.4091	0.3668
50	0.62	3.4689	0.00019	0.4731	0.3287
60	0.72	3.8597	0.00021	0.5279	0.2961
75	0.88	4.5020	0.00024	0.5968	0.2551
90	1.02	5.2136	0.00026	0.6529	0.2217
105	1.16	6.0021	0.00028	0.6993	0.1941
120	1.30	6.8810	0.00030	0.7382	0.1709
150	1.56	8.9408	0.00032	0.7992	0.1346
180	1.81	11.4845	0.00034	0.8441	0.1079
210	2.05	14.6121	0.00035	0.8777	0.0879
240	2.29	18.4736	0.00036	0.9034	0.0726
300	2.74	29.1242	0.00038	0.9388	0.0515
360	3.18	45.2487	0.00038	0.9607	0.0385

APPENDIX E

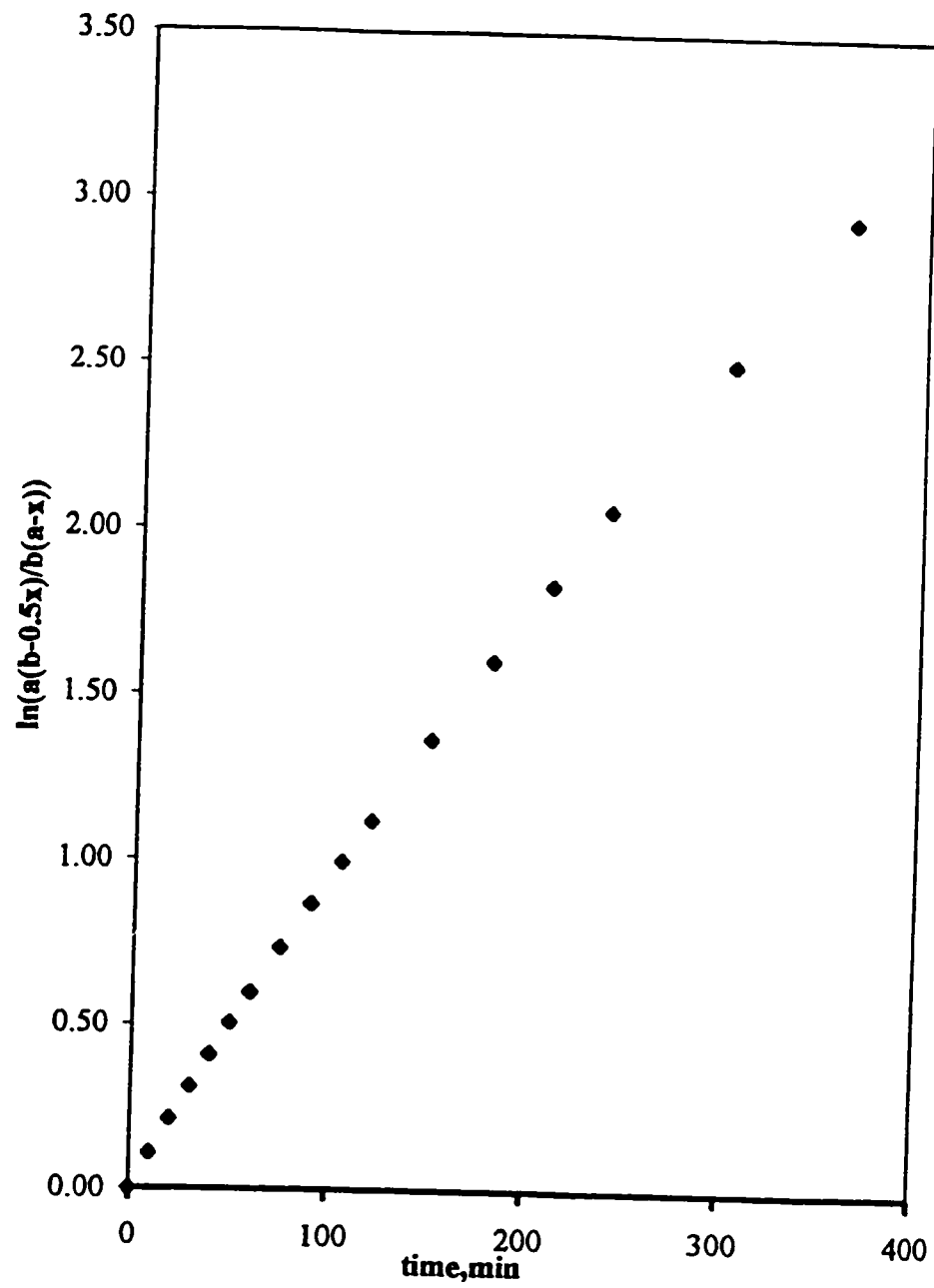
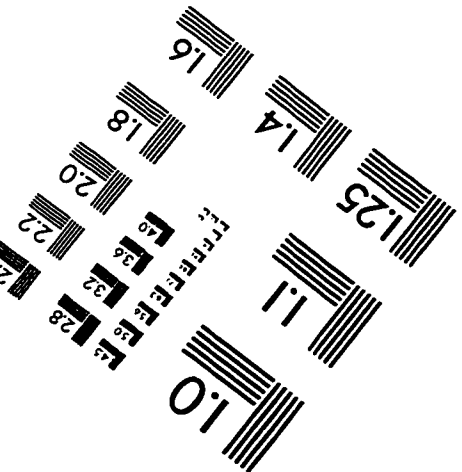
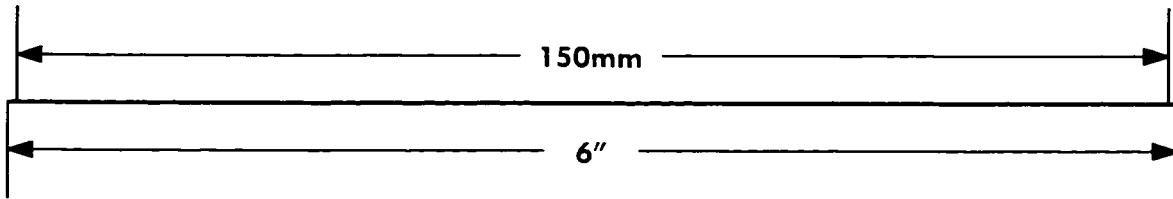
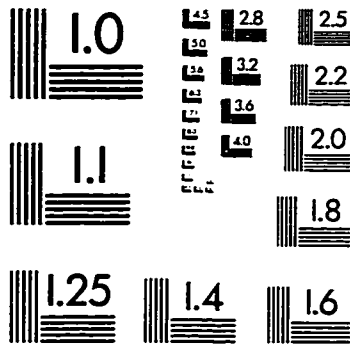
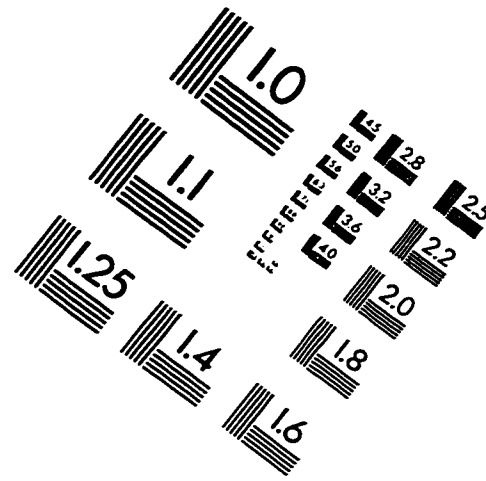
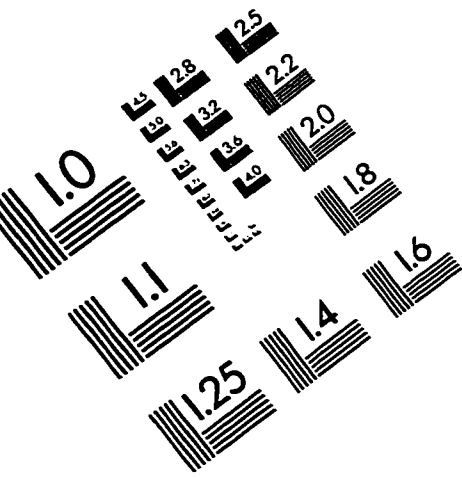


Figure 16. Plot of $\ln(a(b-x)/b(a-0.5x))$ against time.

IMAGE EVALUATION TEST TARGET (QA-3)



APPLIED IMAGE, Inc.
1653 East Main Street
Rochester, NY 14609 USA
Phone: 716/482-0300
Fax: 716/288-5989

© 1993, Applied Image, Inc., All Rights Reserved

